INTERFACE

royalsocietypublishing.org/journal/rsif

Review

Cite this article: Ambrosi D, Ben Amar M, Cyron CJ, DeSimone A, Goriely A, Humphrey JD, Kuhl E. 2019 Growth and remodelling of living tissues: perspectives, challenges and opportunities. *J. R. Soc. Interface* **16**: 20190233.
http://dx.doi.org/10.1098/rsif.2019.0233

Received: 29 March 2019
Accepted: 26 July 2019

Subject Category:
Reviews

Subject Areas:
bioengineering, biomathematics, biomechanics

Keywords:
growth, remodelling, living systems, morphoelasticity, instabilities

Authors for correspondence:
Jay D. Humphrey
e-mail: jay.humphrey@yale.edu
Ellen Kuhl
e-mail: ekuhl@stanford.edu

THE ROYAL SOCIETY
PUBLISHING

Growth and remodelling of living tissues: perspectives, challenges and opportunities

Davide Ambrosi[1], Martine Ben Amar[2], Christian J. Cyron[3,4], Antonio DeSimone[5], Alain Goriely[6], Jay D. Humphrey[7] and Ellen Kuhl[8]

[1]Dipartimento di Matematica, Politecnico di Milano, Milan, Italy
[2]Laboratoire de Physique Statistique, Ecole Normale Supérieure, Paris, France
[3]Institute of Continuum Mechanics and Materials, Hamburg University of Technology, Hamburg, Germany
[4]Institute of Materials Research, Helmholtz-Zentrum Geesthacht, Geesthacht, Germany
[5]Scuola Internazionale Superiore di Studi Avanzati, Trieste, Italy
[6]Mathematical Institute, University of Oxford, Oxford, UK
[7]Department of Biomedical Engineering, Yale University, New Haven, CT, USA
[8]Department of Mechanical Engineering, Stanford University, Stanford, CA, USA

DA, 0000-0003-2952-9613; MBA, 0000-0001-9132-2053; JDH, 0000-0003-1011-2025; EK, 0000-0002-6283-935X

One of the most remarkable differences between classical engineering materials and living matter is the ability of the latter to grow and remodel in response to diverse stimuli. The mechanical behaviour of living matter is governed not only by an elastic or viscoelastic response to loading on short time scales up to several minutes, but also by often crucial growth and remodelling responses on time scales from hours to months. Phenomena of growth and remodelling play important roles, for example during morphogenesis in early life as well as in homeostasis and pathogenesis in adult tissues, which often adapt to changes in their chemo-mechanical environment as a result of ageing, diseases, injury or surgical intervention. Mechano-regulated growth and remodelling are observed in various soft tissues, ranging from tendons and arteries to the eye and brain, but also in bone, lower organisms and plants. Understanding and predicting growth and remodelling of living systems is one of the most important challenges in biomechanics and mechanobiology. This article reviews the current state of growth and remodelling as it applies primarily to soft tissues, and provides a perspective on critical challenges and future directions.

1. Introduction

Biological cells, tissues, organs and organisms exhibit a remarkable ability to grow by changing their mass and remodel by changing their internal structure. Growth and remodelling enable normal development and somatic growth, they drive adaptations to changes in external stimuli, and they mediate many responses to injury, disease and therapeutic interventions. In many cases, growth and remodelling processes depend strongly on mechanical factors and the associated mechanobiological response at the cellular level. Experience throughout the past three decades reveals that mathematical modelling of growth and remodelling processes can provide valuable insight into the basic biology and physiology, help guide the design and interpretation of appropriate experiments, and inform planning for therapeutic intervention. In this review, we discuss some of the historical and conceptual foundations upon which theories of growth and remodelling have emerged and provide illustrative examples of their use, focusing mainly on soft tissues. We conclude by identifying future challenges and opportunities.

1.1. Historical background

Scientific interest in using mechanics to understand fundamental aspects of biological systems dates back at least to the beginnings of modern science itself

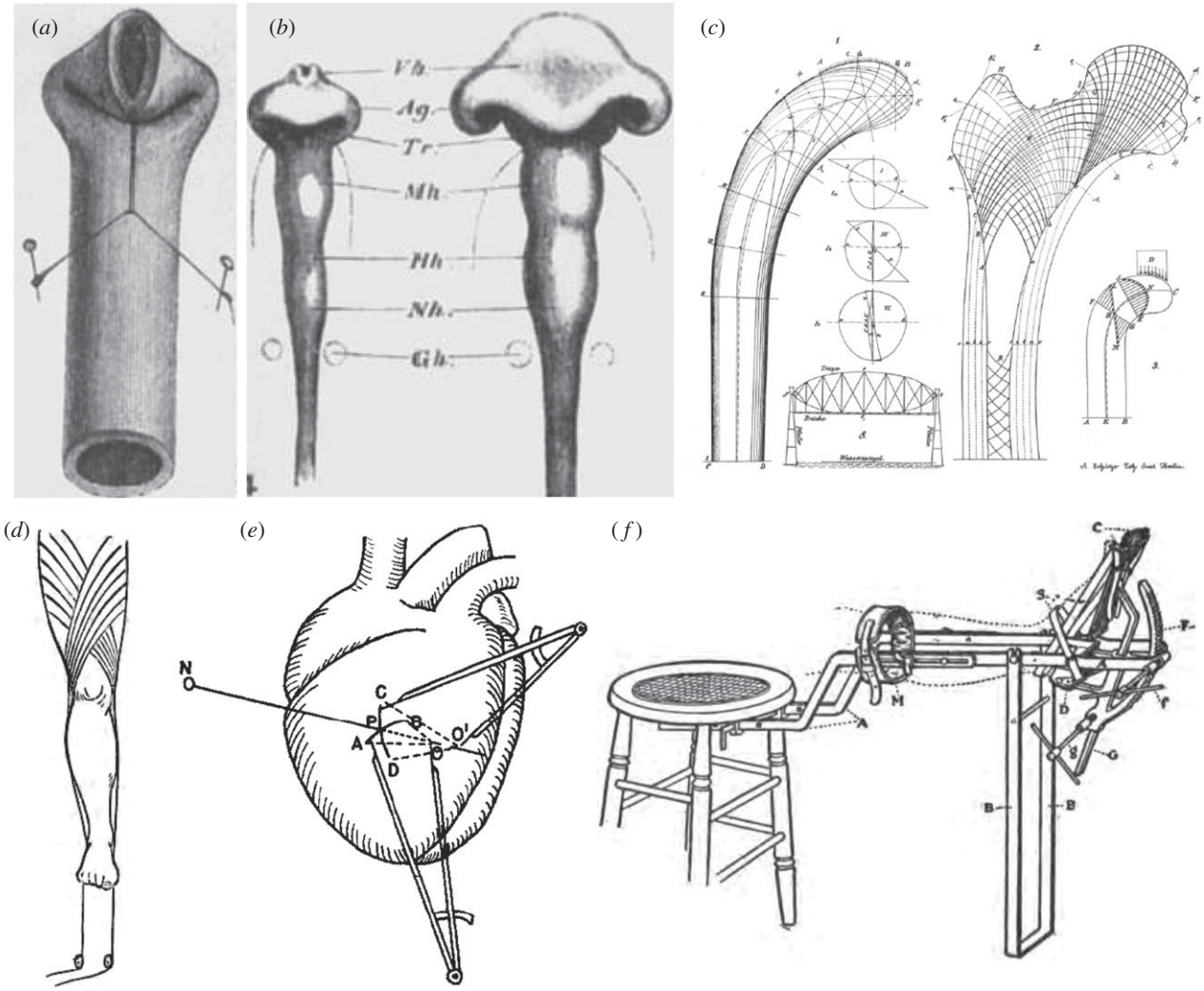

Figure 1. A golden age of discovery and invention in growth and remodelling: Wilhelm His's mechanical analogy between (*a*) the folding of a rubber tube and (*b*) the folding of a gut tube during morphogenesis [1]. (*c*) Wolff's structural study of a bone [2]. (*d*) Traction methods by Davis to exploit mechanical homeostasis [3]. (*e*) Woods' study of the heart (from Burton [4]). (*f*) Joseph Nutt's innovative techniques such as a traction shoe to help elongate the gastrocnemius muscle [5] were based on the idea that stress influences growth and remodelling in soft tissues and bones. Adapted from [6].

and some early examples are summarized in figure 1. While Galileo Galilei (1564–1642) was interested in the strength of bones, particularly in the optimal strength-to-weight relation in animals of different sizes, a true recognition of the role of mechanics in biological growth and remodelling only took place towards the end of the nineteenth century. Specifically, after some initial work, the period between 1867 and 1893 marks a golden age of growth mechanics with scientists from multiple disciplines observing, discussing and employing simple relationships between forces acting on growing organs and organisms and their overall response in terms of shape evolution or mass addition. In short order, scientists postulated new laws of physiology such as Davis's law of soft tissue remodelling, Wolff's law for bones and Woods' law for the heart that paved the way to modern studies in biomechanics and mechanobiology [3–5]. These studies address different physiological systems, and include morphogenesis. The influential work of the Swiss anatomist Wilhelm His, in a series of essays on *Unsere Körperform* and *Entwicklungsmechanik*, suggested that developmental mechanics is a key driver for shaping organs and, in particular, is necessary to explain the characteristic folding pattern of our brain [7]. Following this early period, amply discussed in the monumental 1917 book *On Growth and Form* by Sir D'Arcy Thompson [8], interest of the biological community shifted to the biochemical and genetic components of growing organisms. It was thus not until the 1960s, with the rise of quantitative physiology and biomedical engineering, especially the modern field of biomechanics, that mechanics again became a main object of interest in the context of growth and remodelling.

An important modern contribution to the field of growth and remodelling of bone was the theory of adaptive elasticity in the 1970s [9–11]. This work distinguishes hard tissue growth via appositional, surface-based processes from soft tissue growth via interstitial, volume-based processes. Soon thereafter, an alternate approach for studying growth focused primarily on large strain kinematics to describe changes in size and shape [12,13], which motivated the theory of finite kinematic or volumetric growth. Several groups built upon these ideas, with an elegant conceptual approach for soft tissues put forward in a seminal publication in 1994 [14]. This theory has been adopted by many and is described in detail below. Alternatively, several other approaches evolved based on rate-dependent formulations for soft tissues using the concept of evolving stress-free natural configurations and evolving microstructural changes that affect macroscopic stiffness [15]. At about the same time, in the mid-1990s, it was recognized that growth and remodelling mechanics

Table 1. A brief history of concepts and mechanics related to tissue growth and remodelling (adapted from [6]).

year	scientist	study
1638	Galileo	first discussion of scaling in biomechanics
1832	Bourgery	connection between bone and mechanics
1867	Davis	law for soft tissue remodelling
1870	Wolff	mathematical law for bone design
1874	His	Unsere Körperform und das Physiologische
1880	Roy	nonlinear response, pre-stretch in arteries
1881	Roux	functional adaptation principle applied to bone
1888	His	principles of animal morphology
1892	Woods	mechanical role of wall stress in heart
1893	Thoma	remodelling of arteries
1913	Nutt	diseases and deformities of the foot
1917	D'Arcy Thompson	growth and form
1926	Cannon	concept of homeostasis
1947	Kleiber	metabolic rate scaling with mass
1976	Cowin and Hegedus	adaptive elasticity to describe bone growth
1981	Skalak and colleagues	nonlinear elasticity to describe growth
1987	Frost	mechanostat for bone
1988	Murray, Maini and Tranquillo	elastic models for wound healing
1993	Fung	mass–stress relations
1994	Rodriguez, Hoger and McCulloch	theory of finite growth
1995	Taber	key review on growth modelling
2002	Humphrey and Rajagopal	constrained mixture relations

should include mass–stress relations that account for changes in the production or removal of material in response to changes in loads [16]. Motivated by these ideas and by an increased appreciation of the different mechanical properties and rates of turnover of different extracellular matrix components, a theory of constrained mixtures was proposed in 2002 [17], which is also described in more detail below. Others similarly adopted concepts from the continuum theory of mixtures, though employing other approaches [18–21]. Table 1 provides a brief summary of some of the key discoveries that connect growth and mechanics.

1.2. Biomechanics versus mechanobiology

Biomechanics is the development, extension and application of the principles and methods of mechanics for studying problems of biology and medicine. Modern continuum biomechanics emerged in the mid-1960s following advances in nonlinear continuum mechanics and rapidly grew with advances in computational methods and computer technology, which enabled solution of complex initial-boundary value problems as well as the performance and interpretation of complex biomechanical experiments. Mechanobiology is the study of biological responses by cells to mechanical stimuli. Modern mechanobiology emerged in the mid-1970s following advances in mammalian cell culture and molecular and cell biology, noting that many biological responses to changes in the mechanical environment of the cell are mediated by changes in gene expression. While biomechanics includes diverse areas ranging from protein folding to gait analysis, continuum biomechanics focuses on cells, tissues and organs and naturally complements studies in mechanobiology: one exploits advances in mechanics and the other advances in biology, while both seek to understand questions of structure–function relationships and growth and remodelling throughout the cycle of life. Some of the first observations of mechanobiological responses in mammalian cells were in vascular cells: endothelial cells are very responsive to local blood flow-induced wall shear stress, which is typically of the order 1.5 Pa, while vascular smooth muscle cells are very responsive to blood pressure-induced intramural stress, which is typically of the order of 150 kPa. Clearly, therefore, different cell types can respond to very different magnitudes of imposed loads, in this case differing by five orders of magnitude. Indeed, this comparison reminds us that computed values of stress can be important mechanobiologically even if negligible biomechanically. Mechano-sensitive cells include other myocytes, chondrocytes, fibroblasts, macrophages and osteoblasts, to name a few [22]. Fibroblasts, for example, differentiate into myofibroblasts in response to increased stress and the cytokine transforming growth factor-beta. Like differentiated cells, stem cells also respond to their mechanical environment. Stem cell fate, that is, differentiation, can be driven in part by the stiffness of the matrix on which or in which the cells reside [23]. In general, progressively increasing stiffness tends to drive mesenchymal stem cells towards an adipocyte, myocyte, chondrocyte or osteoblast phenotype, respectively. Not surprisingly then, many cell types actively mechano-sense and mechano-regulate the extracellular matrix, which is facilitated by transmembrane proteins,

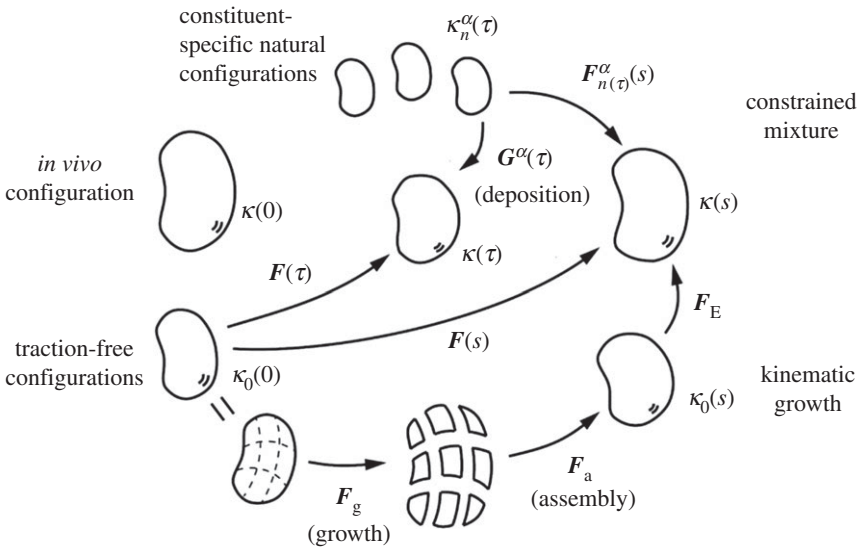

Figure 2. Schematic drawing of evolving configurations of importance in both a theory of finite kinematic growth (bottom portion) and a constrained mixture theory (top portion). In particular, note the common reference $\kappa_o(0)$ and current $\kappa(s)$ configurations. In the kinematic growth theory, one imagines that infinitesimal stress-free portions of the body grow independently via the transformation $\boldsymbol{F}^{\mathrm{g}}$, which need not result in compatible growth. An elastic 'assembly' transformation $\boldsymbol{F}^{\mathrm{a}}$ ensures a contiguous traction-free body, which typically is residually stressed. Finally, an elastic load-dependent transformation $\boldsymbol{F}^{\mathrm{E}}$ yields the current configuration of interest, with $\boldsymbol{F}^{\mathrm{e}} = \boldsymbol{F}^{\mathrm{E}} \cdot \boldsymbol{F}^{\mathrm{a}}$ that part of the deformation that is elastic and determines the stress field. Conversely, in the constrained mixture theory, it is the constituent-specific deformation $\boldsymbol{F}^{\alpha}_{n(\tau)}$ from an individual stress-free configuration that dictates the elastic stress within that constituent. It is easy to show that $\boldsymbol{F}^{\alpha}_{n(\tau)}(s) = \boldsymbol{F}(s) \cdot \boldsymbol{F}^{-1}(\tau) \cdot \boldsymbol{G}^{\alpha}(\tau)$, where $\boldsymbol{G}^{\alpha}(\tau)$ is a so-called 'deposition stretch' tensor that accounts for cells depositing new extracellular matrix under stress when incorporating it within stressed extant matrix. Both approaches require multiplicative deformations, one in terms of the prescribed growth of stress-free elements and one in terms of a deformation that is built into individual constituents when they are incorporated within extant tissue.

notably integrins, that connect the extracellular matrix to the cytoskeleton that includes actin and myosin filaments that allow active force sensing or application [24]. There is, therefore, a pressing need to understand the mechanobiology—the transduction, transcription and translation of mechano-chemical information—and to mathematically model these pheonomena [25]. We now understand that many biological cells, tissues and organs exhibit a mechanical homeostasis, namely a tendency to maintain or restore a preferred mechanical state. When perturbed from this state, cells tend to engage mechanobiological processes to relax themselves or the associated extracellular matrix back to the preferred state. This behaviour is conceptually similar to stress relaxation in viscoelasticity or the tendency towards thermomechanical equilibrium though achieved via active cell-mediated rather than just innate physio-chemical processes. Similar to studies of stability in thermomechanics, much can be learned by studying the mechanobiological stability.

2. Theory of finite growth

The theory of finite growth was first formalized in the mid-1990s [14] and rapidly gained popularity with the use of computational methods to solve the underlying set of governing equations [26]. In contrast to the traditional theory of finite elasticity that consists of the classical set of kinematic, balance and constitutive relations, the theory of finite kinematic growth requires two additional sets of equations: kinematic and kinetic equations of growth [27]. Those two relations have to be prescribed constitutively to close the system of governing equations and thus are specific to the type of physiological system—the brain [28,29], the vasculature [30], the gut [31,32], the airways of the lung [33], the skin [34,35] or the heart [36]. The theory of finite growth is based on a particular multiplicative decomposition of the deformation gradient. Consider a motion $\boldsymbol{\varphi}: \mathcal{B}_0 \to \mathcal{B}_t$ that maps an initial reference configuration $\mathcal{B}_0$ to a current configuration $\mathcal{B}_t$ via $\boldsymbol{x}(\boldsymbol{X}, t) = \boldsymbol{\varphi}(\boldsymbol{X}, t)$, where $\boldsymbol{x}(\boldsymbol{X}, t)$ is the position at time t of the material point originally located at $\boldsymbol{X}$ at time $t = 0$. The main idea is to decompose the deformation gradient, $\boldsymbol{F} = \nabla \boldsymbol{\varphi} = \partial \boldsymbol{x}/\partial \boldsymbol{X}$, into an elastic part $\boldsymbol{F}^{\mathrm{e}}$ and a growth part $\boldsymbol{F}^{\mathrm{g}}$ [14,37]

$$\boldsymbol{F} = \boldsymbol{F}^{\mathrm{e}} \cdot \boldsymbol{F}^{\mathrm{g}}. \tag{2.1}$$

The growth tensor $\boldsymbol{F}^{\mathrm{g}}$ effectively represents the addition or the subtraction of mass to a local volume element. We typically prescribe $\boldsymbol{F}^{\mathrm{g}}$ constitutively, either directly or in rate form to characterize the evolution of growth. Typically, only the elastic contributions $\boldsymbol{F}^{\mathrm{e}}$ generate mechanical stresses. Figure 2 illustrates that we can understand growth via a series of stress-free configurations. In the simplest case, we can assume a stress–strain behaviour of neo-Hookean type with Cauchy stress

$$\boldsymbol{\sigma} = [\lambda \ln(\det(\boldsymbol{F}^{\mathrm{e}})) - \mu]\boldsymbol{I} + \mu \boldsymbol{F}^{\mathrm{e}} \cdot (\boldsymbol{F}^{\mathrm{e}})^{\mathrm{t}}, \tag{2.2}$$

where λ and μ are the elastic Lamé constants and $\boldsymbol{I}$ is the second-order identity tensor. Similar to the classical theory of finite elasticity, this stress enters the linear momentum equation in equilibrium

$$\mathrm{div}(\boldsymbol{\sigma}) + \rho \boldsymbol{b} = 0, \tag{2.3}$$

where ρ is the overall mass density and $\boldsymbol{b}$ is the body force. Provided we know the growth tensor $\boldsymbol{F}^{\mathrm{g}}$, we can solve this equation, with appropriate boundary conditions, either analytically for simple geometries or numerically using nonlinear finite-element solvers. A defining feature of the theory of finite growth is the series of *incompatible* growth configurations expressed mathematically by the growth tensor $\boldsymbol{F}^{\mathrm{g}}$. Importantly, the growth tensor is not necessarily a gradient of a

vector field. Physically, this implies that, once grown, the initial pieces of a living system may become incompatible and may no longer fit together [38]. Figure 2 illustrates that these pieces must be deformed elastically to remain a continuum without openings or overlaps, which results in growth-induced *residual stresses*. These residual stresses can arise from differential growth and are a hallmark of living tissues that fulfil many functions. We can easily visualize the existence of residual stresses through the classical opening angle experiment by introducing a radial cut in an isolated arterial ring [39]. In the developing brain, differential growth is increasingly recognized as one of the major factors that modulates the complex surface morphology of the cerebral cortex [40]. Representing growth and remodelling via the multiplicative decomposition of the deformation gradient poses a number of interesting mathematical questions. For a hyperelastic material characterized by a strain energy functional W, we can parametrize this functional as $W(\boldsymbol{F}^{\mathrm{e}}) = W(\boldsymbol{F} \cdot \boldsymbol{F}^{\mathrm{g}-1})$, recalling that the growth tensor $\boldsymbol{F}^{\mathrm{g}}$ has to be defined constitutively [41]. In the following, we revisit the mathematical properties of $W(\boldsymbol{F}^{\mathrm{e}})$ to understand the consequences of growth $\boldsymbol{F}^{\mathrm{g}}$.

2.1. Material frame indifference

This guiding principle requires that constitutive relations remain invariant under changes in the frame of reference, e.g. that material properties are independent of superimposed rigid-body motions. This implies that

$$W(\bar{\boldsymbol{F}}^{\mathrm{e}}) = W(\boldsymbol{F}^{\mathrm{e}}) \quad \text{with } \bar{\boldsymbol{F}}^{\mathrm{e}} = \boldsymbol{Q} \cdot \boldsymbol{F}^{\mathrm{e}} \quad \forall\, \boldsymbol{Q} \in \mathrm{SO}(3), \tag{2.4}$$

where $\boldsymbol{F}^{\mathrm{e}} = \boldsymbol{F} \cdot (\boldsymbol{F}^{\mathrm{g}})^{-1}$ and SO(3) is the group of all rotations about the origin of three-dimensional Euclidean space. To *a priori* satisfy this requirement, we can select strain energy functionals W with an explicit dependence on the elastic right Cauchy–Green deformation tensor $\boldsymbol{C}^{\mathrm{e}}$

$$\begin{aligned} W(\bar{\boldsymbol{C}}^{\mathrm{e}}) &= W(\boldsymbol{C}^{\mathrm{e}}) \quad \text{with } \bar{\boldsymbol{C}}^{\mathrm{e}} \\ &= (\boldsymbol{Q} \cdot \boldsymbol{F}^{\mathrm{e}})^{\mathrm{t}} \cdot (\boldsymbol{Q} \cdot \boldsymbol{F}^{\mathrm{e}}) \quad \forall\, \boldsymbol{Q} \in \mathrm{SO}(3), \end{aligned} \tag{2.5}$$

where $\boldsymbol{C}^{\mathrm{e}} = (\boldsymbol{F}^{\mathrm{e}})^{\mathrm{t}} \cdot \boldsymbol{F}^{\mathrm{e}} = (\boldsymbol{F}^{\mathrm{g}})^{-\mathrm{t}} \cdot \boldsymbol{F}^{\mathrm{t}} \cdot \boldsymbol{F} \cdot (\boldsymbol{F}^{\mathrm{g}})^{-1}$. We immediately realize that our constitutive choice for the Cauchy stress (2.2) satisfies the requirement of material frame indifference *a priori*.

2.2. Material symmetry

This consideration of symmetry is more subtle. Physically, for an isotropic material, unless growth itself is isotropic, the overall response of the material need not remain isotropic. The problem is then to find the transformation of a given material symmetry group $\mathcal{G}$ for $W(\boldsymbol{F}^{\mathrm{e}})$ in the presence of growth. To determine the material symmetry group, we notice that if $\boldsymbol{Q} \in \mathcal{G}$, a linear transformation belonging to the group of symmetry of the grown material [42], then

$$\begin{aligned} W(\boldsymbol{F} \cdot (\boldsymbol{F}^{\mathrm{g}})^{-1}) &= W(\boldsymbol{F} \cdot (\boldsymbol{F}^{\mathrm{g}})^{-1} \cdot \boldsymbol{Q}) \\ &= W(\boldsymbol{F} \cdot (\boldsymbol{F}^{\mathrm{g}})^{-1} \cdot \boldsymbol{Q} \cdot \boldsymbol{F}^{\mathrm{g}} \cdot (\boldsymbol{F}^{\mathrm{g}})^{-1}). \end{aligned} \tag{2.6}$$

This identity tells us that the material symmetry group after the growth-remodelling process is the conjugate of $\mathcal{G}$ through $\boldsymbol{F}^{\mathrm{g}}$, $\bar{\mathcal{G}} = \{(\boldsymbol{F}^{\mathrm{g}})^{-1} \cdot \boldsymbol{Q} \cdot \boldsymbol{F}^{\mathrm{g}};\, \boldsymbol{Q} \in \mathcal{G}\}$. We should keep this in mind when considering the growth and remodelling of an anisotropic material. A remarkable example is a transverse isotropic material when $\boldsymbol{F}^{\mathrm{g}}$ is a rotation itself: the symmetry axis rotates as it occurs in the reorientation of trabeculae in the bones.

2.3. Thermodynamics

A crucial point of the multiplicative $\boldsymbol{F}^{\mathrm{e}} \cdot \boldsymbol{F}^{\mathrm{g}}$ decomposition is the form of the tensor $\boldsymbol{F}^{\mathrm{g}}$ that gives rise to a biomechanically expected behaviour. A reinterpretation of the classical dissipation inequality of continuum mechanics in open systems [43–45] can help to determine a suitable growth law. An energetic characterization of the dissipative nature of the growth process can suggest thermodynamically admissible evolution laws. However, we must take great care when using thermodynamics. While the entropy inequality can provide useful guidelines in closed systems, it often does not provide valuable information in open systems that may contain entropy sinks. Early thermodynamic considerations identified the Mandel stress and the Eshelby stress as key quantities in formulating growth laws [43,46]. They also identify two types of growth processes [6]: first, *passive growth processes* during which the dissipation inequality is satisfied even in the absence of entropy sinks. This situation is typical for physical systems and arises, for instance, in plasticity, thermoelasticity or gel swelling, where a non-compliant entropy contribution is not required for the process to take place [47]. The observed macroscopic response is then slaved to the overall dissipation mechanism. This type of growth is not incompatible with physical processes. Second, *active growth processes*, during which case an additional sink of entropy must be included to satisfy the dissipation inequality. This situation arises in many biological systems where the cell, through its genetic information and internal energy contribution, can alter the entropy of a system by forcing a pre-programmed response to external stimuli, against the physical increase of entropy. Therefore, active processes at the microscopic level must be at work, and, indeed, are key to the organization of highly organized structures in a dissipative environment [48].

2.4. Differential geometry

From a geometric perspective, the deformation gradient is a map from the tangent space of a point in a reference configuration to the tangent space of the same point in a current configuration. In classic nonlinear elasticity, a convenient measure of changes in distances and angles is the *right Cauchy–Green tensor*

$$\boldsymbol{C} = \boldsymbol{F}^{\mathrm{t}} \cdot \boldsymbol{F}. \tag{2.7}$$

In the presence of growth, the tensor $\boldsymbol{F}^{\mathrm{g}}$ maps the tangent space at each point of the initial configuration to the tangent space of a virtual stress-free state. The equivalent to the Cauchy–Green tensor, now associated with growth,

$$\boldsymbol{C}^{\mathrm{g}} = (\boldsymbol{F}^{\mathrm{g}})^{\mathrm{t}} \cdot \boldsymbol{F}^{\mathrm{g}}, \tag{2.8}$$

acts as a metric for the intermediate virtual configuration. The problem is now that the union of all the tangent spaces forms a tangent bundle that defines this intermediate configuration. But this configuration is not clearly defined. An alternative approach is to start with a reference configuration that is not Euclidean and to characterize inelastic effects such as growth by the intrinsic geometry. The natural structure to achieve equivalence between a theory of multiple configurations and a non-Euclidean theory is a *Weitzenböck manifold* [49,50]. In this framework, the reference configuration is a material manifold

with a vanishing curvature tensor but with a torsion tensor $\mathcal{T}$ defined by the growth tensor $\boldsymbol{F}^{\mathrm{g}}$

$$\mathcal{T}(\boldsymbol{F}^{\mathrm{g}}) = \boldsymbol{F}^{\mathrm{g}-1}\,\mathrm{skw}(\nabla \boldsymbol{F}^{\mathrm{g}}), \tag{2.9}$$

where skw(°) defines the skew-symmetric part of a tensor (°), defined by $\mathrm{skw}(T)_{kij} = T_{kij} - T_{kji}$ in a Cartesian basis. We can then formally define the intermediate configuration that is routinely used in finite inelasticity as a Weitzenböck manifold with torsion tensor $\mathcal{T}(\boldsymbol{F}^{\mathrm{g}})$ and its tangent bundle is the natural space on which we can define all kinematic quantities of the theory with distorsions, e.g. morphoelasticity, thermoelasticity or elasto-plasticity. This *a posteriori* justification of the classical morphoelasticity approach provides a rigorous way to answer fundamental questions on the mathematical nature of growth processes. Borrowing ideas from the geometric theory of defects in solids, we can further generalize the theory to introduce new effects associated with growth- and remodelling-localized point or line growth. These effects require a generalization of the Weitzenböck manifold to include non-vanishing curvature and non-metricity [49,51,52]. Using differential geometry also opens the door to developing new numerical schemes that take advantage of the underlying geometric structure [53]. Another interesting difficulty arises when considering the dynamic evolution of growth. If we assume that the growth tensor $\boldsymbol{F}^{\mathrm{g}}$ depends on the stress, the torsion is determined by a set of partial differential equations involving torsion itself. The evolution of the geometry and topology of manifolds through differential equations, such as Ricci flows [54], is an important topic of differential geometry that is of direct relevance to the mathematical description of kinematic growth. Taken together, the theory of differential geometry provides an elegant theoretical basis for growth and remodelling of a single constituent. However, in a theory of mixtures, multiple constituents with different reference configurations are mixed and the underlying structure of the material manifold is less obvious. Much work must be done in this regard to elucidate key foundational aspects of a mixture theory.

2.5. Surface growth

In this review, we focus primarily on volume growth, which assumes an addition or subtraction of mass within regions of existing tissue. Alternatively, tissues may grow by surface growth, which assumes an addition of material at the tissue surface Γ. Typical examples are growing horns [55], tusks [30], shells [56] or bones [57]. Surface growth models also often adopt a multiplicative decomposition of the deformation gradient, $\boldsymbol{F} = \boldsymbol{F}^{\mathrm{e}} \cdot \boldsymbol{F}^{\mathrm{g}}$, into an elastic part $\boldsymbol{F}^{\mathrm{e}}$ and a growth part $\boldsymbol{F}^{\mathrm{g}}$, or an additive decomposition of the material velocity $\boldsymbol{V} = \boldsymbol{V}^{\Gamma} + \boldsymbol{V}^{\mathrm{g}}$ into the surface velocity $\boldsymbol{V}^{\Gamma}$ and the velocity of the grown material $\boldsymbol{V}^{\mathrm{g}}$ [30].

2.6. Analysis

Independently of the geometric nature of the governing equations, we can formulate the problem of growth either as a variational problem with respect to the modified strain-energy density function or as a set of nonlinear partial differential equations. Representing growth through a set of partial differential equations allows us to establish valuable results on well posedness and local existence of solution [58], which give hope that general global results will follow. A natural question to ask is how the classical problems of elasticity extend to morphoelasticity. For instance, there exist several classes of universal solutions for isotropic materials [59]. In the case of compressible, isotropic materials, a complete generalization of the classic problem of Ericksen is possible [60], but the case of incompressible isotropic materials is still open. Once the existence of such solutions is established, we can study general bifurcation and stability phenomena for problems that involve both mixed boundary conditions and varying growth parameters.

3. Theory of constrained mixtures

The continuum theory of mixtures is a logical starting point for modelling many aspects of cell, tissue and organ growth and remodelling since processes and properties differ by cell type and extracellular matrix constituent. For example, actin and intermediate filaments polymerize/depolymerize at different rates within an adapting cell; elastic and collagen fibres have different half-lives in the extracellular matrix [17,24]. Yet, a full mixture theory is complicated by numerous factors, including the difficulty of quantifying momentum exchanges between constituents within nonlinear solids and specifying how traction conditions partition on boundaries, especially in the presence of evolving mass or microstructure. Motivated by Fung's call for mass–stress relations, a theory of constrained mixtures was proposed to exploit advantages of a mixture theory while avoiding inherent complexities [17]. This approach allows us to model different mechanical properties, rates of turnover and natural configurations of the different constituents.

3.1. Mass–stress relations

In a continuum theory of mixtures, we first consider mass balance for a mixture of $\alpha = 1, 2, \ldots, N$ structurally significant constituents

$$\frac{\partial \rho^{\alpha}}{\partial s} + \mathrm{div}(\rho^{\alpha} \boldsymbol{v}^{\alpha}) = \bar{m}^{\alpha}, \tag{3.1}$$

where ρ^{α} is the spatial mass density, $\boldsymbol{v}^{\alpha}$ is the velocity and $\bar{m}^{\alpha}$ is the net rate of mass density production or removal, which we must prescribe constitutively. It can depend on various chemical or mechanical factors, including stress and the growth and remodelling time s. Three assumptions for a constrained mixture theory of growth and remodelling are: first, that individual constituents can have separate natural, stress-free configurations, but they are constrained to move with the mixture as a whole, $\boldsymbol{x}^{\alpha} \equiv \boldsymbol{x}$; second, that growth and remodelling are typically slow relative to rates of mechanical loading, $\dot{\boldsymbol{x}}^{\alpha} = \boldsymbol{v}^{\alpha} \equiv \boldsymbol{v} \cong \boldsymbol{0}$; third, that the net rate of mass production of removal can be modelled via a multiplicative decomposition $\bar{m}^{\alpha} = m^{\alpha} q^{\alpha}$, where $m^{\alpha}(\tau) > 0$ is the true rate of mass production and $q^{\alpha}(s, \tau) \in [0, 1]$ is a survival function that tracks that part of the constituent produced at growth and remodelling time $\tau \in [0, s]$ that remains at current time s. These assumptions render mass balance integrable

$$\rho_R^{\alpha}(s) = \rho_R^{\alpha}(0) Q^{\alpha}(s) + \int_0^s m_R^{\alpha}(\tau) q^{\alpha}(s, \tau)\,\mathrm{d}\tau, \quad \rho_R(s) = \sum_{\alpha=1}^{N} \rho_R^{\alpha}(s), \tag{3.2}$$

where the subscript R refers to quantities defined per unit reference volume, for example $\rho_R^{\alpha} = (\det(\boldsymbol{F}))\rho^{\alpha}$, and $Q^{\alpha}(s) \in [0, 1]$ is similar to $q^{\alpha}(s, \tau)$ but for constituents

produced at or before time 0 and having the property that $Q^\alpha(0) = 1$ similar to $q^\alpha(\tau, \tau) = 1$.

3.2. Mechanical stress

To use the classical equation of linear momentum balance (2.3), rather than a full mixture relation that necessarily includes momentum exchanges, we further assume that the Cauchy stress can be determined from a rule-of-mixtures relation for the stored energy per unit reference volume, $W_R = \sum W_R^\alpha$, consistent with a standard constitutive relation of finite elasticity

$$\boldsymbol{\sigma} = \frac{2}{\det(\boldsymbol{F})}\boldsymbol{F}\cdot\frac{\partial W_R}{\partial \boldsymbol{C}}\cdot\boldsymbol{F}^{\mathrm{t}} - p\boldsymbol{I}, \tag{3.3}$$

where $\boldsymbol{F} = \nabla\boldsymbol{\varphi} = \partial\boldsymbol{x}/\partial\boldsymbol{X}$ is the deformation gradient, $\boldsymbol{C} = \boldsymbol{F}^{\mathrm{t}}\cdot\boldsymbol{F}$ is the right Cauchy–Green tensor and p is a Lagrange multiplier that enforces incompressibility during transient motions. The key requirement is a constitutive form for the energy stored in each constituent due to its deposition within extant tissue and its individual deformation. With (3.2), we can posit

$$\rho W_R^\alpha(s) = \rho_R^\alpha(0)Q^\alpha(s)\hat{W}^\alpha(\boldsymbol{C}^\alpha_{n(0)}(s)) + \int_0^s m_R^\alpha(\tau)q^\alpha(s,\tau)\hat{W}^\alpha(\boldsymbol{C}^\alpha_{n(\tau)}(s))\,\mathrm{d}\tau, \tag{3.4}$$

where ρ is the mass density of the mixture, $\hat{W}^\alpha$ are stored energy functions for individual structurally significant constituents that depend on constituent-specific right Cauchy–Green tensors $\boldsymbol{C}^\alpha_{n(\tau)}(s) = (\boldsymbol{F}^\alpha_{n(\tau)}(s))^{\mathrm{t}}\cdot\boldsymbol{F}^\alpha_{n(\tau)}(s)$, with $\boldsymbol{F}^\alpha_{n(\tau)}(s)$ the deformation gradient experienced by an individual constituent α relative to its own natural configuration $\kappa_n^\alpha(\tau)$, which can evolve and is denoted simply by a subscript $n(\tau)$; recall figure 2. Two simple special cases illustrate the motivation for this particular general form. For case 1, consider the special case of no growth and remodelling, namely a normal mechanical behaviour defined within finite elasticity. In this case, $s = 0$ and equation (3.4) reduces to

$$W_R^\alpha(s=0) = \frac{\rho_R^\alpha(0)\hat{W}^\alpha(\boldsymbol{C}^\alpha_{n(0)}(0))}{\rho} = \phi_R^\alpha(0)\hat{W}^\alpha(0), \tag{3.5}$$

which is a simple rule-of-mixtures relation, as desired, with ϕ_R^α a mass fraction. For case 2, consider the special case of *tissue maintenance* wherein tissue turns over continually, with production balancing removal within an unchanging mechanical configuration with unchanging material properties. In this case, the natural configuration is $\kappa_n^\alpha(\tau) \equiv \kappa_n^\alpha(0)$, whereby the constituent-specific strain energy function within the integral does not change with growth and remodelling time $\tau \in [0, s]$

$$\rho W_R^\alpha(s) = \left(\rho_R^\alpha(0)Q^\alpha(s) + \int_0^s m_R^\alpha(\tau)q^\alpha(s,\tau)\,\mathrm{d}\tau\right)\hat{W}^\alpha(\boldsymbol{C}^\alpha_{n(0)}(s)), \tag{3.6}$$

whereby, from equation (3.4) and the definition of the mass fraction, we again recover a simple rule of mixtures.

3.3. Kinematics

Equation (3.4) reveals the need to determine the constituent-specific deformation gradient $\boldsymbol{F}^\alpha_{n(\tau)}(s)$. From figure 2, we can imagine evolving configurations of the mixture from an *in vivo* reference configuration $\kappa(0)$ to an intermediate $\kappa(\tau)$ or final $\kappa(s)$ configuration. We can define deformations associated with these configurations similar to standard finite elasticity, for example $\boldsymbol{F}(\tau)$ and $\boldsymbol{F}(s)$. Importantly, there can be a natural, stress-free configuration at any of these same times for each constituent, from which we can consider the constituent to be deformed when deposited within extant matrix at the time of its synthesis, say $\tau \in [0, s]$. From figure 2, we conclude that

$$\boldsymbol{F}^\alpha_{n(\tau)}(s) = \boldsymbol{F}(s)\cdot\boldsymbol{F}^{-1}(\tau)\cdot\boldsymbol{G}^\alpha(\tau), \tag{3.7}$$

where the linear transformation $\boldsymbol{G}^\alpha$ is the *deposition stretch*; it accounts for cells depositing new constituents with an intrinsic pre-stress, an important aspect of mechanical homeostasis. Interestingly, both the theory of finite growth and the constrained mixture theory require multiplicative decompositions of the motion to account for growth and remodelling according to figure 2. The former requires a growth tensor that depends constitutively on chemo-mechanical stimuli and accounts for rates of change; the latter requires a deposition stretch that plays the role of an internal variable while the rates of change are accounted for by mass production and removal functions.

3.4. Illustrative constitutive relations

Equation (3.4) also reveals that the constrained mixture theory requires three constitutive functions, one for mass production $m_R^\alpha(\tau)$, one for mass removal $q^\alpha(s, \tau)$ and one for the mechanical properties of the existing mass $\hat{W}^\alpha(\boldsymbol{C}^\alpha_{n(\tau)}(s))$. We can define the constituent-specific stored energy functions within the context of finite elasticity and can include neo-Hookean or Fung exponential forms, which are common in tissue biomechanics. Consider, therefore, the relations related to mass turnover. Importantly, many matrix constituents are constantly being produced, elastin being a counter-example, and most cell types are constantly dividing, cardiomyocytes being a counter-example, hence it seems reasonable to posit production in terms of a basal rate as well as changes therein due to chemo-mechanical or other stimuli. It is also known that many processes such as degradation of matrix and death of populations of cells follow first-order-type kinetics, also at basal rates that can be modulated by chemo-mechanical stimuli. We assume that

$$m_R^\alpha(\tau) = m_o^\alpha g(\text{stimuli}) \quad \text{and}$$
$$q^\alpha(s,\tau) = \exp\left(-\int_\tau^s k_o^\alpha f(\text{stimuli})\,\mathrm{d}\tau\right),$$

where m_o^α is an original basal or homeostatic production rate and k_o^α is an original basal or homeostatic rate parameter, with g and f scalar functions that need to be determined constitutively for individual cells and tissues, typically as functions of deviations in mechanical stress or chemical factors from normal values, with $g = 1$ and $f = 1$ at a homeostatic state. We can show that basal homeostatic processes, such as tissue maintenance, further require that basal rates of production and removal balance, for example $m_o^\alpha/k_o^\alpha = \rho_o^\alpha$.

3.5. Remodelling

It is important to emphasize that growth and remodelling often proceed hand in hand. Changes in internal microstructure can arise when old constituents are replaced with new constituents, via degradation and deposition, that have a different orientation, diameter, cross-linking or other characteristic. Modelling this change in cytoskeleton or matrix, which need not involve a change in mass, is thus critical. Indeed, there can also be cases wherein cells remodel tissue microstructure independent of

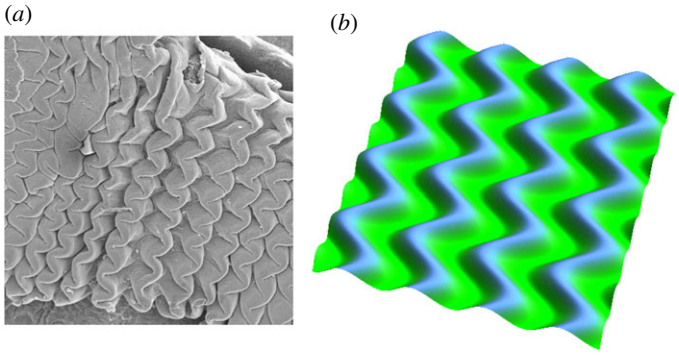

Figure 3. Mechanical instability. Various patterns emerge from multi-layered systems during embryogenesis. Zigzag patterning in pre-villus ridges in the jejunum of turkey embryos (*a*) and simulations using the theory of finite kinematic growth (*b*) show the importance of mechanical instabilities in governing shape in morphogenesis. Adapted from [31]. (Online version in colour.)

mass production and removal, that is, by simply refashioning extant matrix, which requires actomyosin activity. Just as the fibroblast is the prototypical synthetic cell, collagen is the prototypical matrix constituent, frequently central to remodelling in adaptations, disease and injury, especially wound healing, wherein the fibroblast differentiates into a myofibroblast. Our commentary here is brief for excellent reviews on cell-mediated collagen remodelling can be found elsewhere [61,62]. Note, however, that matrix orientation defines tissue anisotropy, a key characteristic of matrix mechanics. If the deformation is affine, filament or fibre orientation can be calculated simply from $\lambda \boldsymbol{m} = \boldsymbol{F} \cdot \boldsymbol{M}$, where $\boldsymbol{m}$ and $\boldsymbol{M}$ define the filament or fibre direction in current and reference configurations, respectively, and $\lambda = \sqrt{\boldsymbol{C} : \boldsymbol{M} \otimes \boldsymbol{M}}$ is the filament or fibre stretch. In remodelling, we are interested in changes in orientation separate from those induced simply by deformations. Cell-mediated fibre alignment often results from mechanical stimuli, with cells orienting the fibres along the directions of principal strain, principal stress or some angle between [62]. Different cell types appear to use different rules to dictate such alignment, and it has been shown that testing various hypotheses against known alignments under normal conditions can often be used to identify cell-specific alignment rules as well as relations describing the rate of change of the orientation during remodelling. The interested reader is referred to the aforementioned reviews or some key papers [63–65].

3.6. Additional implementations

Various direct uses of this constrained mixture theory range from modelling aneurysmal enlargement [66] and cerebral vasospasm [67] to the *in vivo* development of tissue-engineered constructs [68]. The associated computational implementation is expensive owing to the heredity integrals and the need to store past histories, thus multiple methods have been developed to render the method more computationally tractable. One is a simple reduction of the modelling to consider only an initial and a single perturbed state, thus eliminating the need for the heredity integrals [69,70]. Other methods have included a temporal homogenization to yield rate equations [71] and a concept of mechanobiological equilibration [72]. In addition, there are many other mixture-based models of biological growth and remodelling, some of which include methods of finite kinematic growth coupled with the concept of a constrained mixture. The interested reader is referred to the many other examples of mixture-based theories, including a study of cartilage growth [18], a model of tumour growth [19], a general framework for growth [73], growth in tissue engineering [74], a study of residual stress [21], a new multi-generational theory of growth [75], a focus on mass transfer within growth mechanics [76], hypertensive remodelling of arteries [77], development of the aorta [78], a study of diverse applications including cervical remodelling in pregnancy [79], a coupling of haemodynamics and arterial wall growth and remodelling [80], additional studies of tissue engineering [81,82], anisotropic volumetric remodelling [83] and asthmatic airway remodelling [84], to name a few.

4. Mechanical instabilities

An interesting mechanism through which biological shape can develop is a mechanical instability resulting from prior growth [37,85]. For example, if different parts of a tissue grow at different rates, they can build sufficient stresses to create a mechanical instability similar to the well-known Euler buckling instability [86]. For instance, the shapes of multiple organs arise as a direct result of growth and remodelling during early development. This period of embryonic or fetal life, dominated by cell proliferation and tissue formation, gives multiple examples of pattern formation via buckling and post-buckling induced by growth as illustrated in figure 3.

Each part of our body is structured in multiple adjacent layers that had experienced growth and remodelling. With very simple modelling of volumetric growth, we can explain the development of various structures in our body, from circumvolutions of the basal membrane that separates the dermis from the epidermis [34] to the undulations of our small intestine [31] or the convolutions that define our brain. These patterns are not only amazing structures, they also play a role in physiology: dips are the location of adult stem cell niches in our skin or small intestine; defects in brain circumvolutions, localized or not, induce severe pathologies of newborns [87]. Typically, the time scale associated with the growth process is very long compared with the visco-elasticity of the sample. This implies that, from the biomechanical point of view, the structure always remains in equilibrium and can be modelled using the minimization of a free energy. Variational methods in finite elasticity with volumetric growth are powerful tools to analytically investigate pattern formation; they establish not only the instability threshold, the so-called control parameter in the theory of bifurcations, but also the first nonlinearities. Figure 4 shows that, in the simple geometry of a slab subjected to growth in one direction, the Biot instability [88] predicts a periodic pattern without

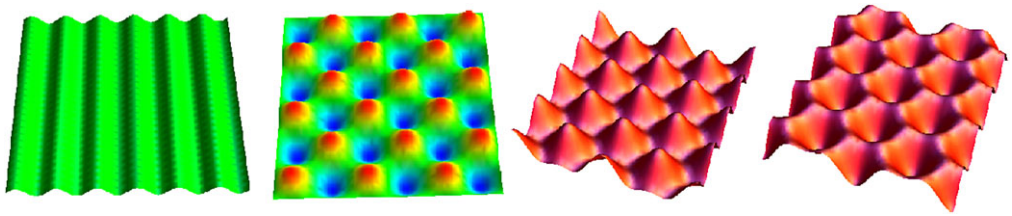

Figure 4. Mechanical stability. Only small changes can induce large variations in pattern formation and the generation of shape. Typical undulations obtained after buckling instability include stripes, chessboards, hexagon+ and hexagon− patterns. Adapted from [90]. (Online version in colour.)

specification of the geometry: stripes, squares or two families of hexagons depending on their centre elevation. Even for neo-Hookean elasticity, a weakly nonlinear analysis establishes that the selected pattern is indeed the pattern that is observed experimentally [89].

One approach is based on defining an energy density in terms of invariants I_1, I_2, I_3 that in turn depend on the deformation gradient $\boldsymbol{F} = \partial \boldsymbol{x}/\partial \boldsymbol{X}$. Again using $\boldsymbol{F}^{\mathrm{e}} = \boldsymbol{F} \cdot \boldsymbol{F}^{\mathrm{g}-1}$, the basic strategy consists of minimizing the free energy of the system under constraints. These constraints include incompressibility, as commonly applied in biomechanics. Surface energies, as, for example, from capillarity, compete with the boundary conditions deduced from the variational process

$$\mathcal{E} = \int_V \frac{[x_X^2 + y_Y^2 + \tau^2(x_X^2 + y_Y^2) - 2 - 2p(J-1)]}{\tau}\, \mathrm{d}X\, \mathrm{d}Y,$$

where p is a Lagrange parameter enforcing two-dimensional incompressibility, and $\tau = \vartheta_1/\vartheta_2$ where ϑ_1 and ϑ_2 are eigenvalues of the two-dimensional growth tensor $\boldsymbol{F}^{\mathrm{g}} = \mathrm{diag}\{\vartheta_1, \vartheta_2\}$, which are monotonically increasing functions in time. Growth implies that $\vartheta_1, \vartheta_2 > 1$. Stresses originate at borders due to connections to other tissues, as well as due to anisotropic or heterogeneous growth. As growth proceeds, stresses increase in the sample and, being compressive, can induce bifurcations that are revealed with this method. In complex geometrical systems that are incompressible and involve several layers, directly eliminating the Lagrange parameter p helps to render the system of nonlinear partial differential equations tractable. This is also why the introduction of a nonlinear stream function can be helpful [34]. As in viscous two-dimensional hydrodynamics, this function allows us to solve the Euler–Lagrange equations derived from the free energy, though it is restricted to systems that can be reduced to two dimensions and do not develop fully three-dimensional instability patterns. Variational methods may also include viscoelasticity. Motivated by cyclic tensional tests, which are commonly performed to study living tissues [91,92], and inspired by the difficulty of generalizing the classical one-dimensional Maxwell and Kelvin–Voigt models of linear viscoelasticity into the nonlinear regime, the Rayleighian method turns out to be especially powerful [93,94]. Without difficulty, this method provides the correct formulation of dissipative tensors, which have been a matter of extensive debates in the acoustic domain [95].

5. Mechanobiological instabilities

Whereas the growth-induced instabilities discussed in the prior section refer to possible instabilities of mechanical equilibria that arose from prior growth and remodelling, there is also a need to study possible instabilities of the actual growth and remodelling process itself over long periods. When growth and remodelling arises from mechanobiological responses by cells, we can refer to this analysis as one of *mechanobiological stability* [96], which we can, of course, extend to include responses to biochemical or other stimuli as well. We recall that most biological cells continually reorganize, produce or degrade their surrounding extracellular matrix, often resulting in different geometries and properties. There exist special configurations wherein the net effects of these cellular processes cancel so that these configurations persist over long periods—such configurations are called homeostatic and thus represent mechanobiological equilibria. A key question is whether such equilibria are stable, that is, if they can be maintained despite particular perturbations. It appears that, in healthy adults, most tissues typically maintain their geometry and mechanical properties for many years despite myriad perturbations in diet, exercise and external stimuli, including brief infections, hence suggesting mechanobiological stability under normal cases. Natural ageing, disease progression and responses to injuries, however, can be very different; they may reflect a compromised homeostasis and in some cases mechanobiological instability. Theories of finite growth and mixture-based theories can both be used to examine growth and remodelling related stabilities. For example, consistent with ideas from §2, consider a growth law of the form [97]

$$\boldsymbol{F}^{\mathrm{g}-1} \cdot \dot{\boldsymbol{F}}^{\mathrm{g}} = \boldsymbol{K} : (\boldsymbol{\sigma} - \boldsymbol{\sigma}^{\mathrm{h}}), \tag{5.1}$$

where the dot represents the material time derivative, $\boldsymbol{F}^{\mathrm{g}}$ is a growth tensor that effectively characterizes geometric consequences of local changes in mass in evolving stress-free configurations, and $\boldsymbol{K}$ is a fourth-order tensor characterizing the growth response rate to differences in Cauchy stress $\boldsymbol{\sigma}$ from homeostatic values $\boldsymbol{\sigma}^{\mathrm{h}}$. In this case, mechanobiological equilibrium is defined by $\dot{\boldsymbol{F}}^{\mathrm{g}} = 0$, whereas mechanical equilibrium is enforced implicitly by using values of stress from equilibrated mechanical solutions. In a simple two-dimensional case, for example, we obtain two first-order differential equations of the form $\dot{\gamma}_i = f_{ij}(\boldsymbol{K}, \boldsymbol{\sigma})\gamma_j$. We can conduct a usual stability analysis by considering $\gamma_i = \gamma_i^{\mathrm{eq}} + \epsilon\bar{\gamma}_i$, where the superscript $^{\mathrm{eq}}$ denotes equilibrium values and the overbar denotes perturbations, with $\epsilon \ll 1$. Eigenvalues of the associated Jacobian matrix dictate the mechanobiological stability as indicated in figure 5.

Studies using the constrained mixture theory of §3 similarly use methods from dynamical systems, for example stability analyses, but in terms of different characteristic equations [96,98–100]. In particular, consistent with equations (3.2)–(3.4), the focus turns towards rates of change in mass (equivalently, referential mass density $\rho_R = (\det \boldsymbol{F})\rho = (\det \boldsymbol{F}) \sum \rho^{\alpha}$) and stress, with mechanobiological equilibrium requiring both mass densities and associated mechanically equilibrated stresses to remain unchanged during the period of interest [72,96]. Dynamic stability analyses around these equilibria thus

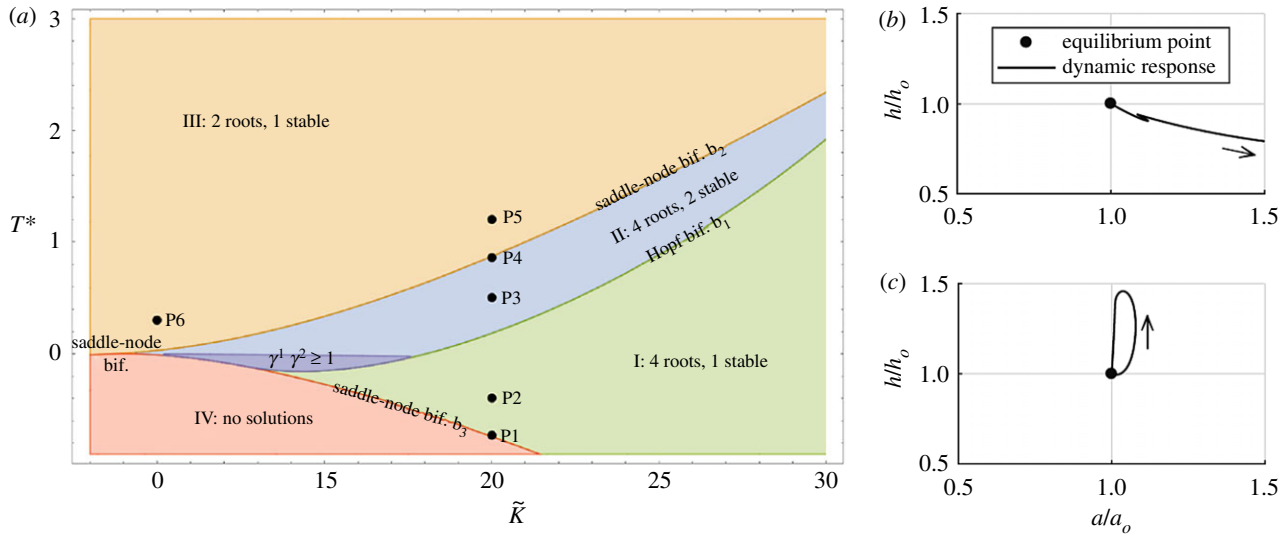

Figure 5. Mechanobiological stability. Phase diagram (*a*) showing distinct regions with different equilibrium states and stability behaviours for a growing tubular structure as a function of its homeostatic stress and anisotropy [97]. Phase-plane-type plots (*b*,*c*) showing both unstable, for a low value of a parameter governing the rate of matrix synthesis (*b*), and asymptotically stable, for a higher value of this parameter (*c*), growth and remodelling responses of an artery (normalized wall thickness h versus luminal radius a) following a transient perturbation in blood pressure [98]. (Online version in colour.)

generally require us to consider equivalent nonlinear evolution equations for mass and stress in rate form. For example, in a simple two-dimensional case, we can derive a non-autonomous system of first-order differential equations for mass density and in-plane stresses for a mixture of the form [98]

$$\dot{\boldsymbol{y}}(s) = [f](\boldsymbol{y}(s), s) \quad \text{and} \quad \boldsymbol{y} = [\rho_R, \sigma_1, \sigma_2]^{\mathrm{t}}. \tag{5.2}$$

The growth and remodelling time $s \geq 0$, with $s = 0$ representing a homeostatic state denoted by superscript h, which requires $\boldsymbol{\sigma}(0) = \boldsymbol{\sigma}^{\mathrm{h}}$. Importantly, we can examine both mechanobiologically static and dynamic stability analogous to static (e.g. limit point bifurcations) and dynamic (e.g. self-excited) mechanical stability. Similar to the volumetric growth approach, we seek stable and unstable solutions given small perturbations of the form $\boldsymbol{y}(0) = \boldsymbol{y}^{\mathrm{h}} + \delta\boldsymbol{y}^{\mathrm{h}}$, which can be examined from an eigenvalue analysis of the associated linearized, autonomous system of differential equations. Depending on the formulation and type of perturbation, one can identify neutral [96,100] or asymptotically [98] stable mechanobiological solutions, the latter consistent with clinical experience that many normal growth and remodelling processes appear to preserve homeostatic states over long periods. Studies have shown that many parameters affect the mechanobiological stability, including but not limited to the level of homeostatic intramural and wall shear stresses, the intrinsic material stiffness and mass density of the tissue or its constituent parts, the associated rates of matrix synthesis and degradation, the presence or not of muscle contractility, and so forth (figure 5). Such insight could be useful in better understanding disease progression or healing following injury, particularly with regard to possible palliative clinical treatments. For example, antagonizing a particular microRNA can hasten collagen production by mesenchymal cells, and simulations show that such increases could slow the rate of enlargement of certain arterial aneurysms [96]. Given the recent recognition that many disease processes involve biological instabilities associated with positive feed-back loops [101], there is continuing motivation to study mechanobiological and related instabilities.

6. Applications

Mathematical models and computational simulations of growth and remodelling have been widely used to study myriad problems ranging from cellular mechano-sensing to developmental biology, understanding disease progression and engineering tissue replacements. In this section, we highlight a few representative examples to show the depth and breadth of these efforts. For each case, we identify problem-specific constitutive relations. In constrained mixture theories, we must identify problem- and constituent-specific constitutive relations for rates of mass production $m_R^\alpha > 0$ and survival $q^\alpha(s, \tau) \in [0, 1]$ and stored energy $\hat{W}^\alpha(\boldsymbol{C}^\alpha_{n(\tau)}(s))$. In the finite growth theories, we can define the growth kinematics to be isotropic, e.g. in tumours or in the brain, with $\boldsymbol{F}^{\mathrm{g}} = \vartheta\boldsymbol{I}$, transversely isotropic along a specific direction $\boldsymbol{n}$, e.g. in skeletal or cardiac muscle, with $\boldsymbol{F}^{\mathrm{g}} = \boldsymbol{I} + [\vartheta - 1]\boldsymbol{n} \otimes \boldsymbol{n}$, or orthogonal to a specific direction $\boldsymbol{n}$, e.g. in skin, with $\boldsymbol{F}^{\mathrm{g}} = \vartheta\boldsymbol{I} + [1 - \vartheta]\boldsymbol{n} \otimes \boldsymbol{n}$, or completely arbitrary [30]. In these examples, ϑ is a growth parameter that follows specific kinetic definitions. In the simplest case, growth is purely morphogenetic, which implies that the evolution of ϑ is independent of physical factors [102]. In tumours or tissue engineering, however, growth depends primarily on the availability of nutrients, and we have to account for nutrient supply [103]. In many other living systems, growth is controlled by the mechanical environment, through shear stresses or pressure in the vascular system, through the area stretch in skin [35] or through the fibre stretch in skeletal muscle [104]. A classical everyday example is the chronic shortening of the gastrocnemius muscle in women who frequently wear high-heeled footwear, as highlighted in figure 6. In the following, we consider a variety of illustrative examples of tissue growth and remodelling. Of course, given the vast number of possible examples and methods, this list is necessarily limited. As noted above, we do not consider growth and remodelling of bone, plants, sea life, etc. Moreover, we focus on continuum theories, noting that other approaches exist as well, including agent-based models [106,107] and stochastic lattice-based models [108,109].

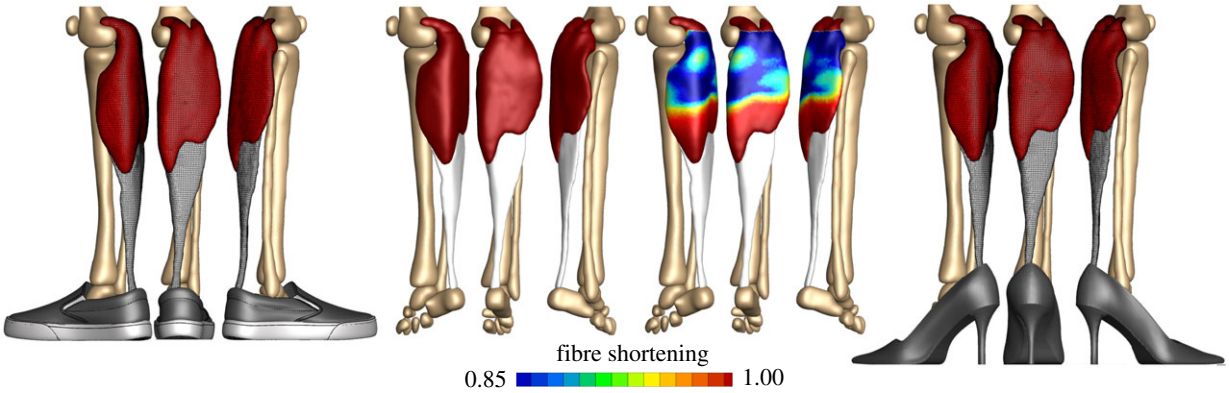

Figure 6. Application to skeletal muscle. Skeletal muscle can lengthen and shorten in response to sustained stretch. A classical everyday example is the chronic shortening of the gastrocnemius muscle in women who frequently wear high heels. The muscle shortens by a chronic loss of sarcomeres, which results in chronic muscle fatigue and an increased injury risk. Adapted from [105]. (Online version in colour.)

6.1. Motility: understanding active movement and locomotion

Motility refers to the ability to move spontaneously and actively. Animal locomotion, which is powered by the contractility of skeletal muscle, is part of the story while, at the level of individual cells and biological tissues, motility is related to cell migration, the immune system response, the establishment of neuron synapses and even wound healing. More broadly, motility is fundamental to both the generation of life and the propagation of diseases, for example through unicellular swimming of sperm, bacteria, parasites and invasion of metastatic tumour cells, as well as to many other biological phenomena of great relevance for life. Muscle contraction is at the root of animal locomotion. Active remodelling of muscle tissue is, thus, central in all motility phenomena involving higher organisms. Quoting from the 1924 Linacre lecture of the English physiologist and Nobel laureate C. S. Sherrington: 'To move things is all that mankind can do … for such the sole executant is muscle, whether in whispering a syllable or in felling a forest' [110]. Study of the mechanics of muscle is a large field, and it would be impossible to even scratch its surface in a few lines. Yet, there are a few classical mathematical references that discuss the basic mechanisms [111,112]. The impact of muscle activity and coordination in the study of animal locomotion is also a vast subject. Classical textbooks [113,114] and reviews [115] can provide a starting point. In recent years, the pioneering work 'Studies in animal locomotion' [116] has inspired a renewed interest in the motility of limbless organisms which, in many respects, provide simpler model systems for studying coordination and locomotion. Locomotion arises from the mechanical interactions of an active elastic body with its surroundings, driven by the action–reaction principle. Muscle activity selects a preferred state of deformation, the configuration that the body would acquire in the absence of external forces. Modulating this state of spontaneous deformation in time in the presence of a surrounding medium, e.g. a fish waving a fin, generates reactive forces from the environment. These can be frictional ground forces in the undulatory locomotion of snakes [117] and in the peristaltic locomotion of worms [118], or viscous and inertial forces from a surrounding fluid in the cases of swimming and flying [119–121], which can be exploited as propulsive forces. Growth is the engine of some distinctive forms of single cell motility. Indeed, while most forms of biological motility are powered by molecular motors, which could be viewed as instances of motility by remodelling, since the steps executed by molecular motors are nothing but chemically activated conformational changes, actin polymerization is a distinctive engine for some specific forms of cell locomotion. Examples include the protrusion of lamellipodia of spreading and migrating embryonic cells, and the bacterium *Listeria monocytogenes* that propels itself through its host's cytoplasm by constructing behind it a polymerized tail of cross-linked actin filaments [122–124]. Remarkably, neuronal growth works in a similar manner, with the protrusion of neurites from the main axonal body, which is powered by the polymerization of actin filaments at the neurite tips known as growth cones [125]. To understand how growth of actin fibres can act as the propulsive engine for a crawling cell, it is instructive to look at the propulsion mechanism of non-adherent cancer cells migrating inside a capillary tube [126]. Actin filaments polymerizing at the leading edge protrude the plasma membrane forward at a velocity V in the laboratory frame, positive if forward. At the same time, they are advected backward by a retrograde actin flow at local velocity v in the cell body frame, negative if backward, powered by myosin molecular motors. Friction from the tube walls is described by a force per unit area, $\tau = -\mu(v + V)$, where $\mu > 0$ is the viscous friction coefficient. Balance of force along the tube axis yields

$$0 = -\pi R^2 \alpha V - 2\pi R \mu \int_0^L (v(x) + V)\, \mathrm{d}x,$$

where α is a coefficient for the hydrodynamic resistance due to flow induced in the tube, and R and L are the radius and length of the cell–tube contact, respectively. We denote the average velocity of the actomyosin retrograde flow by $\langle v \rangle := \int_0^L v(x)\, \mathrm{d}x/L$, and solve for the velocity of the leading edge of the plasma membrane V

$$V = -\frac{1}{1 + (\alpha R)/(\mu 2R)} \langle v \rangle.$$

The above equation shows that the velocity is generally intermediate between the value $-\langle v \rangle$, for perfect cell-wall grip, $\mu \to +\infty$, and the value zero, for perfect cell-wall slip, $\alpha = 0$. Motility is relevant also at the sub-cellular level, where it becomes complicated but also fascinating and relatively unexplored in the details of its mechanics. Again, the basic mechanism is remodelling, in the sense of chemically activated conformational changes of complex molecular machines. This includes, for

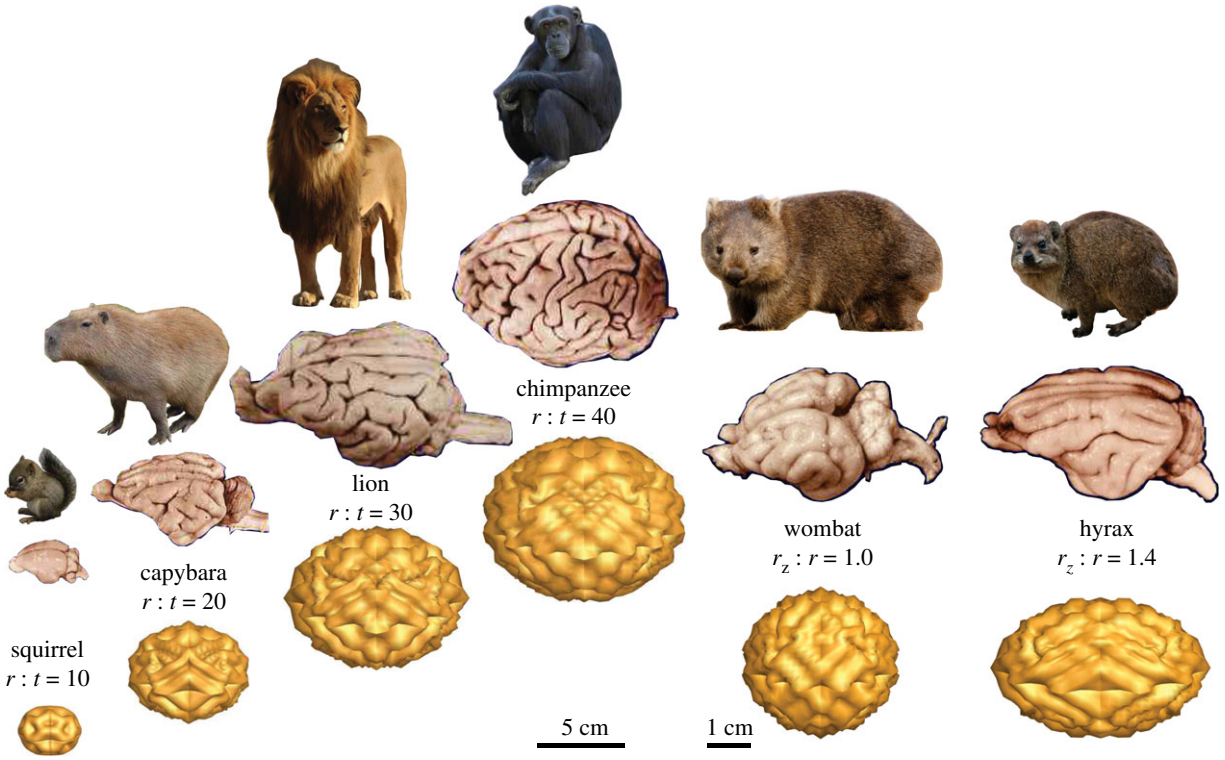

Figure 7. Application to the brain. Differential growth during development creates the characteristic convoluted surface morphology of our brain. By varying the radius-to-thickness ratio $r : t$ or the degree of ellipticity $r_z : r$, mechanical concepts can help explain the varying degrees of complexity of the mammalian brain, for example the brachycephalic, rounded brain of the wombat and the dolichocephalic, elongated brain of the hyrax. Adapted from [40]. (Online version in colour.)

example, the ribosome translating a protein, a molecular process based on the highly coordinated motile behaviour of a nano-scale machine [127]. Understanding the molecular machinery for DNA duplication, editing and transcription, which works in similar ways, is an equally significant problem to explore with the tools of modern mathematics and mechanics.

6.2. The brain: cortical folding during development

One of the most exciting new applications of the theory of growth and remodelling over the last decade has been the systematic study of the geometric features found in the brain. This is not, however, a new topic as the characteristic convolutions of the human brain were first reported in an Egyptian manuscript dated 1700 BC that compares brain convolutions to the corrugations or wrinkles found in molten metal [128]. The description, development and function of these convolutions have also been major topics of research for the last two centuries [87]. The upper part of the convolutions are the *gyri* and the bottom groves are the *sulci*. This folded shape increases the surface area of the brain for a given volume. Functionally, convolutions have the strategic function of increasing the number of neuronal bodies located in the cortex and facilitating the connections between neurons, hence reducing the travelling time of the electric signals between different regions. The mechanism responsible for *gyrification*, the morphogenetic creation of these shapes, is not yet fully understood [129]. However, it is now accepted that intrinsic mechanical forces, rather than external constraints, are responsible for folding in the human brain [130] and recent observational studies [131,132] further support the role of the rapid tangential expansion of the cortex during development as the primary driver for folding [133–136]. Mechanically, the onset of folding can be understood as a build-up of elastic energy in the compressed upper cortex and its partial release by a wrinkling deformation of the film, the grey matter cortex, and substrate, the white matter core. Experimentally, this instability can be reproduced by the constrained polymeric swelling of a circular shell bounded to an elastic disc, which triggers the same type of wrinkling pattern [85,137,138]. Similar experiments performed on a two-layered brain prototype made of polymeric gels with differential swelling properties reproduce folds similar to the gyri and sulci of a real brain [139].

In this simple two-layer system, it is well appreciated that the pattern adopted by the system depends on a number of important factors such as the relative stiffnesses of the two layers [140], the thickness of the thin layer, the growth of the top layer [141], the curvature of the foundation [142], the adhesion energy between the layers [143,144], the imperfection of the substrate [145], the anisotropic response [146,147], the surface tension and pressure [148] and the nonlinear elastic response of the materials [149]. For small ratios of layer μ_l to foundation μ_s stiffnesses, $\mu_l/\mu_s \lesssim 10$, as the wrinkling patterns develop, the system localizes this initial deformation and a fold or crease appears as observed in many biological systems. The deep folding patterns that are formed during the growth of brains are believed to be partially caused by this mechanical instability [87,150]. The analysis of this instability is particularly difficult owing to the existence of multiple unstable linear modes and possible contact. Surprisingly, a complete theoretical description is still lacking and is one of the great challenges of morphoelasticity. For larger ratios of $\mu_l/\mu_s \gtrsim 10$ and sufficient growth, a period-doubling instability occurs due to nonlinearities in the substrate response [151,152], as shown in figure 7. Whereas period doubling is well understood in dynamical systems, understanding the development of a spatial period-doubling pattern is more challenging even in the absence of growth [153]. The theory of growth and

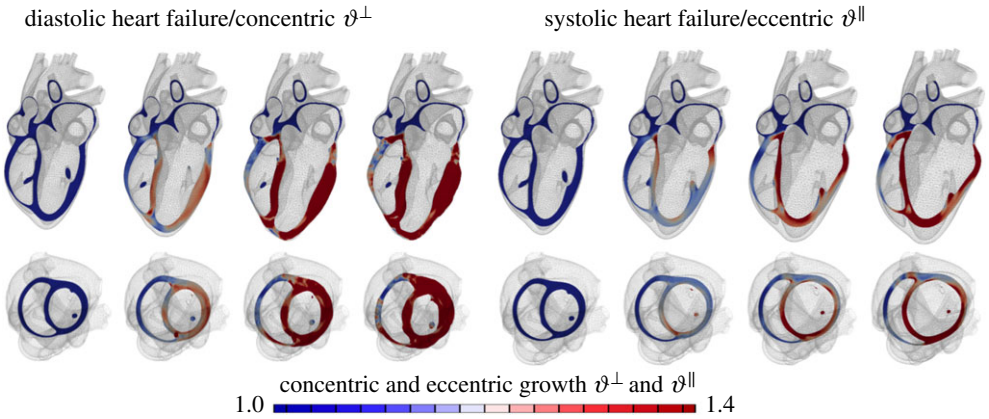

Figure 8. Application to the heart. Our heart responds to a chronic increase in blood pressure by gradual wall thickening and to chronic volume overload by ventricular dilation. Personalized multi-scale models of cardiac growth can predict the time line of cardiac wall thickening in response to local muscle fibre thickening triggered by stresses and of cardiac dilation in response to local muscle fibre lengthening triggered by elevated strains [157]. (Online version in colour.)

remodelling can now be used to explore some of the fine features of this pattern-forming system such as the variation of cortical thickness [154] or the role of initial curvature in aligning primary fissures [155,156].

6.3. The heart: growth and remodelling during heart failure

Chronic heart failure is a medical condition that involves structural and functional changes of the heart and a progressive reduction in cardiac output. Heart failure is classified into two categories: diastolic heart failure, a thickening of the ventricular wall associated with impaired filling; and systolic heart failure, a dilation of the ventricles associated with reduced pump function. We can model both conditions through the multiplicative decomposition of the deformation gradient into an elastic part and a growth part, $\boldsymbol{F} = \boldsymbol{F}^{\mathrm{e}} \cdot \boldsymbol{F}^{\mathrm{g}}$. To model diastolic heart failure through chronic cardiomyocyte thickening, we can introduce a growth multiplier $\vartheta^{\perp}$ that represents the parallel deposition of sarcomeres on the molecular level [36]. The growth tensor for transverse fibre growth follows as the rank-one update of the growth-weighted unity tensor in the plane perpendicular to the fibre direction f_0 as $\boldsymbol{F}^{\mathrm{g}} = \vartheta^{\perp}\boldsymbol{I} + [1 - \vartheta^{\perp}]f_0 \otimes f_0$. The growth multiplier, $\vartheta^{\perp} = \sqrt{\det(\boldsymbol{F}^{\mathrm{g}})} = \sqrt{J^{\mathrm{g}}}$, represents the thickening of the individual muscle cells through the parallel deposition of new myofibrils. To model longitudinal fibre growth through chronic cardiomyocyte lengthening, we can introduce a scalar-valued growth multiplier $\vartheta^{\parallel}$ that reflects the serial deposition of sarcomeres on the molecular level [36]. The growth tensor for longitudinal fibre growth follows as the rank-one update of the unity tensor along the fibre direction f_0 as $\boldsymbol{F}^{\mathrm{g}} = \boldsymbol{I} + [\vartheta^{\parallel} - 1]f_0 \otimes f_0$. The growth multiplier, $\vartheta^{\parallel} = \det(\boldsymbol{F}^{\mathrm{g}}) = J^{\mathrm{g}}$, now takes the physiological interpretation of the longitudinal growth of the individual cardiac muscle cells through the serial deposition of new sarcomere units. This model naturally connects molecular events of parallel and serial sarcomere deposition with cellular phenomena of myofibrillogenesis and sarcomerogenesis to whole organ function. Figure 8 illustrates that our simulation predicts chronic alterations in wall thickness, chamber size and cardiac geometry, which agree favourably with the clinical observations in patients with diastolic and systolic heart failure. A recent longitudinal heart failure study in pigs has shown that changes in sarcomere number alone can explain 88% of myocyte lengthening, which, in turn, can explain 54% of cardiac dilation [158]. This whole heart model can also predict characteristic secondary effects including papillary muscle dislocation, annular dilation, regurgitant flow and outflow obstruction. Computational modelling provides a patient-specific window into the progression of heart failure with a view towards personalized treatment planning.

6.4. Arteries: flow- and pressure-mediated growth and remodelling

Arteries enlarge in response to sustained increases in blood flow, they thicken in response to hypertension, they stiffen in ageing, they change size and shape in aneurysmal dilatation and they assume a dramatically different composition and properties in atherosclerosis. These few cases, and many more, reveal that blood vessels experience significant growth and remodelling in health and disease. Soon after its introduction, the theory of kinematic growth was employed to describe flow- and pressure-mediated growth and remodelling in arteries [159,160]. Combined with a computational solution and patient-specific modelling based on medical images, this approach provides insight into important clinical interventions such as angioplasty and stenting [161]. Yet, like all biological soft tissues, arteries consist of myriad proteins, glycoproteins and glycosaminoglycans. Each has different natural configurations as revealed by early experiments using elastase, collagenase and chondroitinase to selectively degrade individual constituents; each also has different material properties and rates of turnover in the form of synthesis and degradation. In parallel, therefore, different constrained mixture models arose to study arterial growth and remodelling, including predictions of aneurysmal enlargement [67,162] (figure 9). Indeed, such models helped explain the effects of different levels of elastolytic insults versus different rates of collagen deposition on overall rates of lesion enlargement, the latter of which predicted a subsequent experimental finding that suggests the therapeutic potential of antagonizing certain microRNAs to control rates of matrix production. Mixture models similarly allow modelling of separate biomechanical effects of active and passive smooth muscle [163], as well as stimuli other than mechanical, including biochemical effects of thrombus in cerebro-vasospasm [67] or infiltrating inflammatory cells in fibrosis [164]. The former

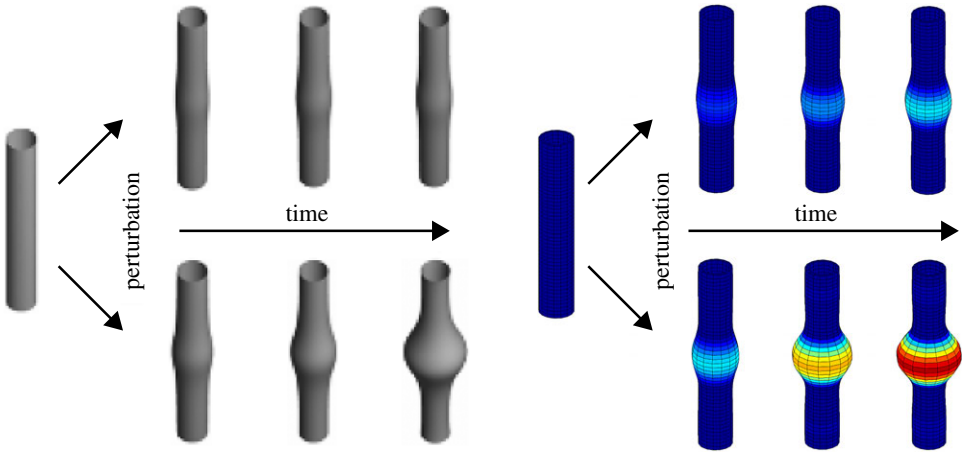

Figure 9. A circular–cylindrical model blood vessel (left) is perturbed by minor damage to its elastin layer. A healthy blood vessel is mechanobiologically stable, and its growth and remodelling will compensate for the damage over time to ensure just a minor permanent change of geometry (top). A diseased blood vessel may be mechanobiologically unstable, and its growth and remodelling can result in an uncontrolled dilatation over time, possibly resulting in aneurysm formation (bottom), depending on many factors, including matrix turnover rates, values of the deposition stretch and so forth [96,98]. (Online version in colour.)

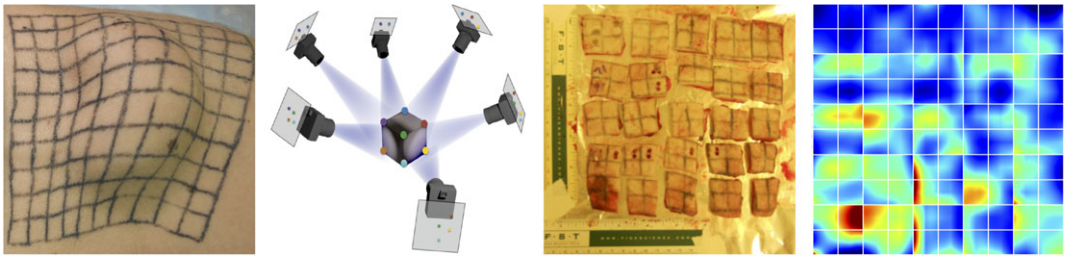

Figure 10. Skin responds to a chronic overstretch by generating new skin, a concept that is frequently used to repair birth defects or burn injuries. Using concepts of multi-view stereo analysis, we can characterize the amount of skin growth from a series of three-dimensional hand-held camera images. Cutting the grown skin into individual pieces in the spirit of figure 2 reveals the effects of differential growth and incompatibility [165]. (Online version in colour.)

accurately predicted the time course of vasospasm and its resolution over a one-month period, revealing that it is rapid collagen turnover, stimulated by extensive growth factors, cytokines and vasoactive substances, in progressively narrowed configurations, not smooth muscle contraction *per se*, that dominates this deadly condition, hence explaining why vasodilators are ineffective therapeutics for vasospasm. The ability to model separately the contributions of individual constituents and their separate growth and remodelling can thus provide important mechanistic insight.

6.5. Skin: growing new skin and fibrosis around implants

Skin is our interface with the outside world. In its natural environment, it displays unique mechanical characteristics including prestrain and growth. While there is general agreement on the physiological importance of these features, they remain poorly characterized mainly because they are difficult to access with standard laboratory techniques. By combining recent developments in multi-view stereo and isogeometric analysis, it is now possible to analyse living skin *in vivo* at virtually no experimental cost [165]. Based on easy-to-create hand-held camera images, we can quantify prestretch, deformation and growth by longitudinally following characteristic anatomic landmarks throughout a chronic skin expansion experiment. Figure 10 shows the gradual inflation of a subcutaneously implanted balloon. By taking weekly photographs of the experimental scene, we can reconstruct the geometry from a tattooed surface grid, and create parametric representations of the grown skin surface. We have analysed these representations using the theory of finite area growth based on the multiplicative decomposition of the deformation gradient $\boldsymbol{F} = \boldsymbol{F}^{\mathrm{e}} \cdot \boldsymbol{F}^{\mathrm{g}}$ into an elastic tensor $\boldsymbol{F}^{\mathrm{e}}$ and a growth tensor $\boldsymbol{F}^{\mathrm{g}} = \sqrt{\vartheta}\boldsymbol{I} + [1 - \sqrt{\vartheta}]\boldsymbol{n} \otimes \boldsymbol{n}$, where ϑ defines the area growth. This model assumes that changes in thickness are purely elastic and no growth takes place in the thickness direction $\boldsymbol{n}$. Surface growth modelling of skin allows us to quantify both the amount of average area prestretch and area growth ϑ as a function of time. We can use these data to calibrate skin growth models and simulate clinical cases of skin expansion; for example, in pediatric forehead reconstruction [35]. These simulations can accurately predict the clinically observed mechanical and structural response of living skin both acutely and chronically. This living skin model can easily be generalized to arbitrary biological membranes and serve as a valuable tool to virtually manipulate living systems, simply by means of changes in their mechanical environment.

Fibrosis around soft implants, e.g. mammary implants, results from a complex inflammatory response [166] characterized by myriad chemical signalling pathways and involves a variety of cells, among them fibroblasts and myofibroblasts. Fibroblasts are the cells that synthesize collagenous fibres of tissues while myofibroblasts are muscle-like cells with active contractile properties [61]. Although fibroblasts exist in any type of tissue, in case of inflammation, new cells are primarily directed towards the allergen source. These cells demonstrate a wounding response to the presence of an implant. Fibrosis

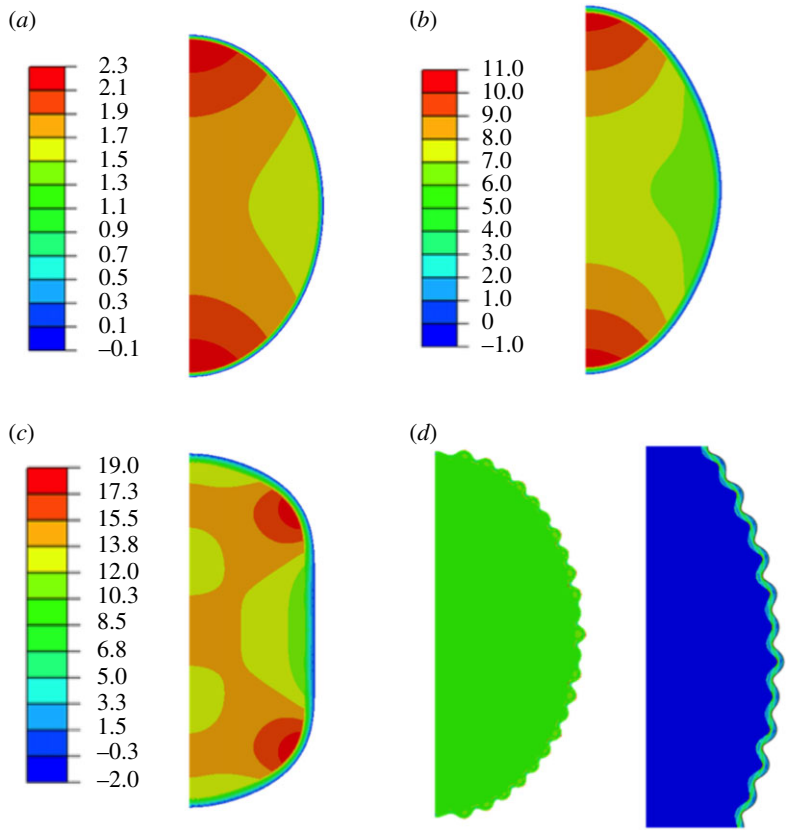

Figure 11. Finite-element simulations of the fibrous capsule in a two-dimensional neo-Hookean model for both implant and capsule. The aspect ratio reflects an implant of radius R and a capsule of order millimetres. In (*a–c*), the stiffness ratio ρ between capsule and implant is 10; in (*d*) it is 100. From (*a*) to (*c*) relative growth per unit length varies from $g = 1.28$ for (*a*), to $g = 1.48$ for (*b*), and $g = 1.60$ for (*c*). For this choice of ρ and g, the outer boundary does not buckle but flattens. The colour code indicates the maximum in-plane stress and demonstrates that the implant is in tension while the capsule is in compression. In (*d*), $\rho = 100$, $g = 1.18$ and we observe buckling. Magnification on the right shows the resulting deformation more clearly and reveals that stress inhomogeneities occurs only at the interface. (Online version in colour.)

always exists around implants, but can be exacerbated after mastectomy and radiotherapy treatment. This can ultimately lead to withdrawal after only a few months because of unbearable pain. *In situ* rupture of the breast prosthesis is another potential complication, which, due to the implant's composition, usually silicon gels, is not good for a patient. A recent study revealed new insights into the biomechanics of the human capsule [167]: fibrosis manifests itself in the appearance of a thin fibrous layer called a capsule [168]. The thickness of the capsule increases with the grade of the pathology, from 0.5 mm thick in grade II up to 3 mm thick in the more severe cases of grade IV. We can estimate the level of compressive stress within the capsule using the theory of finite kinematic growth. Indeed we can compare the formation of the capsule to the growth of a thin layer attached to a semi-spherical surface. Evaluating the stiffness of fibrotic tissue in a tensile test revealed compressive stresses of the order of 10 MPa [167]. This represents a significant stiffening compared with healthy breast tissue with stiffnesses of the order of 1 kPa [169]. This difference may well explain the pain, although the link between pain and compressive stresses has not been quantified. In addition, this estimation discards the possibility of having active compressive cells as myofibroblasts, which is probable for patients at grade III or IV of the pathology. Because of compressive stresses, we expect a wrinkling instability at the implant–capsule interface. We have modelled the deformation at the interface using a two-dimensional neo-Hookean model for both implant and capsule. Figure 11 shows the implant–capsule interface for low values of growth. Strikingly, although the capsule is in compression in the ortho-radial direction, the implant is mainly in tension, which could potentially explain its failure. In conclusion, after more than 50 years of plastic surgery, no real explanation has been found for the existence of fibrosis around soft implants that affects approximately 30% of patients post radiotherapy.

6.6. Tumour growth: nutrients and stress as regulating factors

Cancer is increasingly responsible for death and disability; it is characterized by accelerated cellular proliferation and local changes in matrix and vascular networks. Studies of *in vivo* growth and remodelling are vital, but so too *in vitro* models of disease. The *multi-cellular spheroid* is a standard *in vitro* mechanobiological system for studying the uncontrolled duplication rate of a tumour cell aggregate [170]. A tumour spheroid is a cluster of cells floating in culture medium, proliferating freely in an environment with abundant nutrients. Malignant cells have lost the ability to self-regulate their number through normal apoptosis, regulated by homeostasis with the environment: they duplicate isotropically in an uncontrolled manner, producing a nearly spherical shape. In the case of free, unconstrained growth, the diameter of the tumour typically exhibits an early exponential growth, followed by linear growth. The transition from one regime to the other is mainly regulated by the availability of nutrients, which, in turn, is driven by diffusion through the

intercellular space. In fact, when the size of the tumour $R(t)$ is smaller than the typical diffusion length, nutrient is available everywhere in the spheroid and the growth is purely volumetric, $\mathrm{d}R^3/\mathrm{d}t \simeq R^3$, and the radius increases exponentially in time, $R \simeq e^t$. Conversely, when the diameter of the spheroid is much larger than the penetration length of the nutrient, growth occurs primarily at the surface, $\mathrm{d}R^3/\mathrm{d}t \simeq R^2$, and radius increases linearly in time, $R \simeq t$. In the intermediate regime, the concentration of nutrients decays exponentially with the radius [171], favouring external over internal proliferation.

A mechanical stress, produced by external loads or geometrical constraints, makes the simple scenario illustrated above more complex. The mechanical influence of external loads on tumour growth was first demonstrated in the late 1990s [172]. Growing cell spheroids in agarose gels revealed that the surrounding material is compressed by the expansion of the inner volume and—by the action–reaction principle—the traction exerted by the gel affects the growth rate of the multi-cell spheroid. Gels can be produced at a tunable stiffness by varying the concentration of the solid phase. An *a priori* mechanical characterization of the gel allows one to calculate the pressure exerted by the gel on the growing spheroid, as a function of the spheroid radius. The major finding of the gel experiments is that the generated stress reduces the final size of the spheroid, with decreased apoptosis and non-significant changes in proliferation [172]. It is therefore clear that a precise determination of the constitutive laws that characterize the mechanical behaviour of a tumour spheroid is a pre-requisite to reliably quantify the stress–growth relationship. Early attempts in this respect assumed that a cell conglomerate behaves like a viscoelastic fluid, able to bear a static load because of its surface tension. At equilibrium, measurements of the curvature of a loaded sample provide the surface tension of the fluid. Alternative studies support the idea that tumours behave like solids [173]. In stress–relaxation experiments of various tumour types in confined compression, all tumours equilibrated at a constant, non-zero stress at the end of the experiment, typical of viscoelastic solids. A second argument supporting the assumption of solid-like constitutive equations is the spatial correlation between stress and apoptosis–mitosis in loaded ellipsoidal spheroids [174]. A non-homogeneous proliferation pattern can be produced only by a solid-like material: a hydrostatic behaviour would generate a state of hydrostatic pressure, independent of position within the sample, whereas a solid behaviour generates high stress concentrates around the tips.

Finally, there is increasing evidence of residual stresses in murine and human tumours [175], similar to the aforementioned observation in arteries. Cutting the tumour azimuthally results in a non-zero opening angle, which is the signature of a solid-like behaviour. Residual stresses are likely to be produced by an inhomogeneous duplication rate of cells and by mechanical interactions between the cells and their extracellular matrix, particularly collagen and hyaluronic acid, that strain the tumour microenvironment. Only solids can sustain residual stress, which can be modelled in multiple ways, including differences in deposition stretches or by the evolution of relaxed configurations produced by incompatible growth [103]. This implies that energy can be stored elastically in the unloaded body only if it behaves like a solid. Strikingly, experiments reveal compressive residual stress with negative opening angles in the centre and a tensile residual stress with positive opening angles in the outer shell of the tumour [175]. This observation seems paradox in terms of availability of nutrient concentrations being larger near the tumour boundary, which would favour proliferation and eventually generate compressive stress. In a later series of experiments, the compression of the spheroid was determined by the concentration of Dextran, a large molecule soluted in the bath [176]. As Dextran molecules can enter neither the cell membrane nor the interstitial space, an imbalance of osmotic pressure at the boundary loads the cellular aggregate. For larger concentrations of Dextran, the diameter of the spheroid grew slower and reached a plateau at smaller radius, in agreement with the initial predictions [172]. While a single cell is almost incompressible in response to the pressure generated by Dextran, the volume of the cell aggregate strongly depends on its hydration, that is, the osmotic pressure [177]. This technology allows a precise control of the mechanical stress: the osmotic pressure at the spheroid interface, the force per unit current surface, is constant in time. Considerable data suggest that a cell aggregate behaves as a binary mixture, or poroelastic material: a fluid phase and a solid phase composed of cells and extracellular matrix. Mathematical modelling of solid tumours as porous deformable media has been addressed in a number of publications [19,178,179]; it is a suitable mechanical framework to account for the coupled dynamics of cells, extracellular matrix and interstitial fluid. The interstitial flow is typically represented by a Darcy-type equation, and the mass exchange among individual phases allows a prediction of tumour growth. In the controlled osmotic pressure experiments with Dextran [176], the theory of porous media offers a transparent explanation for the control of the solid stress in the spheroid. Observing that the diameter of the macromolecules is typically larger than the size of the intracellular pores, we assume continuity of total stress and chemical potential at the spheroid boundary [180]

$$(\boldsymbol{\sigma} - p_{\mathrm{in}}\boldsymbol{I}) \cdot \boldsymbol{n} = -p_{\mathrm{out}}\boldsymbol{n} \quad \text{with} \quad p_{\mathrm{in}} = p_{\mathrm{out}} - \pi,$$

where p_{in} is the pressure of the interstitial fluid, $\pi > 0$ is the osmotic pressure caused by Dextran, $\boldsymbol{\sigma}$ is the Cauchy stress in the cellular aggregate, $\boldsymbol{I}$ is the identity tensor and $\boldsymbol{n}$ is the radially outward pointing normal [181]. According to the above equation, the osmotic pressure only loads the solid phase, in agreement with the observation that the solid stress is not affected by the interstitial fluid pressure [175].

Despite the apparent advancements, a number of open questions remain to be addressed: measurements of pressure as a function of the radial position within a spheroid exhibit a trend that remains to be theoretically explained [177]. Similarly, it is not yet clear whether the reduction in volume in the cellular aggregate occurs because of a reduction of the intercellular space only, or because of self-regulation of the osmotic pressure at a cellular level. Experiments report a sodium efflux from the loaded cells, which could explain a fluid outflow to re-establish the equilibrium of chemical potential [182]. This mechanism of regulation at the cellular level contributes to a macroscopic decrease in the diameter of the spheroid that should, in principle, be distinguished from variations in apoptotic and mitotic rates. This points towards the need for a more precise cell-level interpretation of the observed macroscopic tumour size versus time behaviour.

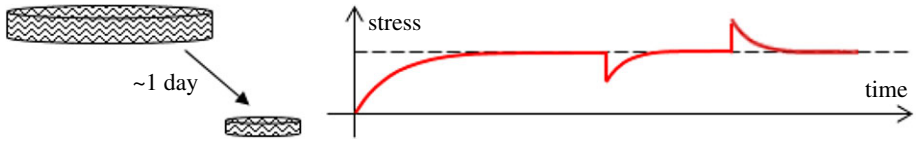

Figure 12. Application to tissue equivalents. Schema of a tissue equivalent being remodelled (compacted) by the embedded cells over a short period in a traction-free environment (left) versus a model-based prediction of remodelling-induced stresses in a cell-seeded uniaxial tissue equivalent, with the homeostatic target stress indicated by the horizontal dashed line and the actual response indicated by the solid curve (right). Note the initial build-up of stress as the cells attempt to compact the gel against fixed end constraints and the subsequent 'relaxation' of stress back towards homeostatic values following either an abrupt release of (first) or increase in (second) the imposed stress. (Online version in colour.)

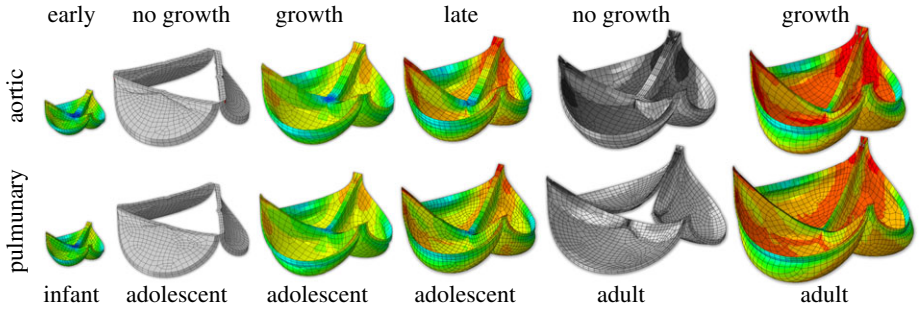

Figure 13. Application to tissue engineering. Characterization of growth during the early and late stages of human heart valve development reveals the amount of leaflet growth that is a mandatory mechanism to prevent regurgitation. Adapted from [190]. (Online version in colour.)

6.7. Tissue engineering: modulating tissues with physical fields

The presence of many diverse confounding factors significantly complicates the identification of key factors that govern biological growth and remodelling *in vivo*. As in the case of studying tumour growth, an interesting way to overcome this problem is to use *in vitro* experiments with so-called tissue equivalents [183]. Tissue equivalents are highly simplified model systems of living tissues. They are typically studied in bioreactors where many relevant factors can be easily controlled. One of the simplest and most widely used experimental set-ups is a free-floating disc of collagen fibres seeded with living fibroblasts and immersed in a culture medium. Within just 24 h, the cells can compact the discs to a fraction of their original diameter [184], a remodelling process that introduces residual stresses [185]. Indeed, similar to the case of spheroids, the stress field is compressive in the interior and tensile in the outer region. To identify the governing principle behind this behaviour, a slightly modified study found that fibroblasts have a natural tendency to remodel the initially relaxed collagen gels towards a state of homeostatic stress [186]. Perturbations of a once established homeostatic state of stress stimulate cells to remodel the matrix until the homeostatic state is restored (figure 12). The notion of a homeostatic stress is well understood in a one-dimensional setting; yet, its three-dimensional generalization remains an open question. Recently developed biaxial experiments with tissue equivalents may help generalize this concept to higher dimensions, which could provide important information for the development and validation of accurate mathematical and computational models of soft tissue mechanobiology [187].

Tissue equivalents are simple model systems of living tissues, mainly suited for academic research. Tissue engineering, by contrast, goes one step further and aims to provide human-made tissue substitutes for clinical applications, for example vascular grafts [188] or heart valves [189]. For example, simulations can quantify the amount of growth required to prevent leakage when tissue engineering valves. Figure 13 shows the effects of somatic growth averaged over $n = 6$ infants, $n = 8$ adolescents and $n = 10$ adults [191] on the aortic and pulmonary valves. Simulations without and with leaflet growth during the early and late stages of development reveal that growth is a natural and mandatory mechanism to prevent regurgitation [190]. Mathematical and computational modelling can help accelerate the expensive experimental and clinical studies that are necessary to push the boundaries in the field of tissue engineering.

Mixture models are particularly useful in this regard since many engineering tissue strategies often use synthetic, biodegradable polymers as scaffolds to promote cell and tissue growth. For example, mixture-based models can be used to examine conditions that affect cell motility and aggregation within scaffolds used in tissue engineering. When focusing on the earliest cellular responses, it can be convenient to assume that the scaffold is rigid and unchanging so as to focus on the interstitial fluid movement, nutrient exchange, and cellular migration or proliferation [74]. Alternatively, scaffold properties are important when considering neotissue production and overall functionality [81]. Because cell-produced neotissue and scaffold necessarily differ in mechanical properties, often with the scaffold consisting of a polymer that degrades, mixture-based models are useful for delineating the separate effects of neotissue turnover and scaffold degradation both *in vitro* and *in vivo* [82,188]. Finally, whereas many successes within tissue engineering have been achieved via extensive trial-and-error empirical studies, mixture-based models promise to aid in scaffold design for one can perform time- and cost-efficient parametric studies and formal optimization using computational models of tissue development [68].

7. Challenges and opportunities

Growth and remodelling are fundamental to most biological processes and considerable progress has been made towards their mathematical understanding. Nevertheless, much remains to be accomplished. Among the many opportunities,

we believe that there is a pressing need for the following. (i) To understand and model the relative influences of genetic, epigenetic and environmental factors on tissue and organ *development*. (ii) To meld increasing information from systems biology models of *cell signalling* within continuum models of growth and remodelling, e.g. a single mechanical stimulus can elicit myriad changes in cell signalling, simultaneously affecting cytoskeletal proteins, cytokine and protease production, and overall matrix integrity. (iii) To account for pathophysiological constraints imposed by *genetic mutations*, e.g. mutations to the gene *FBN1* that codes fibrillin-1, an essential glycoprotein that associates with elastin to increase the long-term biological stability of elastic fibres and compromises the function of many soft tissues. (iv) To expand modelling of mechanobiology to include other effectors, such as *immunobiology* and *pathobiology*. (v) To enable modelling of the effects of specific *pharmacological* treatments on growth and remodelling, e.g. the differential effects of beta-blockers versus angiotensin receptor blockers in the treatment of hypertension. (vi) To increase the computational efficiency of the various growth and remodelling frameworks to enable advanced multi-scale and *personalized* modelling. (vii) To collaborate closely with data scientists to reduce the incredible complexity of biological processes to fundamental laws and rules of growth and remodelling that are amenable to simulation, for example using machine learning and artificial intelligence. Other opportunities exist in the spirit of biomimicry, for example elucidating basic mechanisms of constrained shape optimization and realizing self-healing engineering materials [192,193]. Applications of growth and remodelling thus seem limitless and, with the rapid advancement of medical imaging technologies, personalized simulations seem within reach in the near future. Towards this goal, one of the major challenges in the coming years will be to work hand in hand with biological scientists and clinical researchers to design experiments to rigorously calibrate and validate the requisite evolution equations under physiological and pathological conditions. We hope that this brief review stimulates such advances and many more not yet envisioned.

Data accessibility. This article has no additional data.

Competing interests. We declare we have no competing interests.

Funding. We received no funding for this study.

Acknowledgements. This perspective article stemmed from the Advanced School on 'Growth and Remodelling in Soft Biological Tissue' held 12–16 June 2017 at the International Centre for Mechanical Sciences (CISM) in Udine, Italy, with co-sponsorship provided by the International Union for Theoretical and Applied Mechanics (IUTAM). We acknowledge the tremendous support of CISM in advancing the mechanical sciences through its manifold lectures, textbooks and archival papers, and we dedicate this paper to its many directors and staff.

References

1. His W. 1888 On the principles of animal morphology. *Proc. R. Soc. Edin.* **15**, 287–298.
2. Wolff J. 1870 Über die innere architektur der knochen und ihre bedeutung für die frage von knochenwachstum. *Arch. Pathol. Anat. Physiol. Klin. Med.* **50**, 389–453. (doi:10.1007/BF01944490)
3. Davis HG. 1867 *Conservative surgery*. New York, NY: D. Appleton & Company.
4. Burton AC. 1957 The importance of the shape and size of the heart. *American Heart J.* **54**, 801–810. (doi:10.1016/0002-8703(57)90186-2)
5. Nutt JJ. 1913 *Diseases and deformities of the foot*. London, UK: Forgotten Books.
6. Goriely A. 2017 *The mathematics and mechanics of biological growth*. Berlin, Germany: Springer.
7. His W. 1874 *Unsere Körperform und das physiologische Problem ihrer Enstehung: Briefe an einen Befreundeten Naturforscher*. Leipzig, Germany: FCW Vogel.
8. Thompson DW. 1917 *On growth and form*. Cambridge, UK: Cambridge University Press.
9. Cowin SC, Hegedus DH. 1976 Bone remodeling I: theory of adaptive elasticity. *J. Elast.* **6**, 313–326. (doi:10.1007/BF00041724)
10. Hegedus DH, Cowin SC. 1976 Bone remodeling II: small strain adaptive elasticity. *J. Elast.* **6**, 337–352. (doi:10.1007/BF00040896)
11. Cowin SC, Nachlinger RR. 1978 Bone remodeling III: uniqueness and stability in adaptive elasticity theory. *J. Elast.* **8**, 283–295. (doi:10.1007/BF00130467)
12. Skalak R. 1982 Growth as a finite displacement field. In *Proc. of the IUTAM Symp. on Finite Elasticity* (eds DE Carlson, RT Shield), pp. 347–355. The Hague, The Netherlands: Martinus Nijhoff Publishers.
13. Skalak R, Dasgupta G, Moss M, Otten E, Dullemeijer P, Vilmann H. 1982 Analytical description of growth. *J. Theor. Biol.* **94**, 555–577. (doi:10.1016/0022-5193(82)90301-0)
14. Rodriguez EK, Hoger A, McCulloch AD. 1994 Stress-dependent finite growth in soft elastic tissues. *J. Biomech.* **27**, 455–467. (doi:10.1016/0021-9290(94)90021-3)
15. Tozeren A, Skalak R. 1988 Interaction of stress and growth in a fibrous tissue. *J. Theor. Biol.* **130**, 3370350. (doi:10.1016/S0022-5193(88)80033-X)
16. Fung YC, Liu SQ, Zhou JB. 1993 Remodeling of the constitutive equation while a blood vessel remodels itself under stress. *J. Biomech. Eng.* **115**, 453–459. (doi:10.1115/1.2895523)
17. Humphrey JD, Rajagopal KR. 2002 A constrained mixture model for growth and remodeling of soft tissues. *Math. Model. Methods Appl. Sci.* **12**, 407–430. (doi:10.1142/S0218202502001714)
18. Klisch SM, Chen SS, Sah RL, Hoger A. 2003 A growth mixture theory for cartilage with application to growth-related experiments on cartilage explants. *J. Biomed. Eng.* **125**, 169–179. (doi:10.1115/1.1560144)
19. Byrne H, Preziosi L. 2003 Modelling solid tumour growth using the theory of mixtures. *Math. Med. Biol.* **20**, 341–366. (doi:10.1093/imammb/20.4.341)
20. Ateshian GA. 2007 On the theory of reactive mixtures for modeling biological growth. *Biomech. Model. Mechanobiol.* **6**, 423–445. (doi:10.1007/s10237-006-0070-x)
21. Ambrosi D, Preziosi L, Vitale G. 2010 The insight of mixture theory for growth and remodeling. *ZAMM* **61**, 177–191. (doi:10.1007/s00033-009-0037-8)
22. Wang JHC, Thampatty BP. 2006 An introductory review of cell mechanobiology. *Biomech. Model. Mechanobiol.* **5**, 1–16. (doi:10.1007/s10237-005-0012-z)
23. Discher DE, Mooney DJ, Zandstra PW. 2009 Growth factors, matrices, and forces combine and control stem cells. *Science* **324**, 1673–1677. (doi:10.1126/science.1171643)
24. Humphrey JD, Dufresne ER, Schwartz MA. 2014 Mechanotransduction and extracellular matrix homeostasis. *Nat. Rev. Mol. Cell. Biol.* **15**, 802–812. (doi:10.1038/nrm3896)
25. Vernerey FJ, Farsad M. 2011 A constrained mixture approach to mechano-sensing and force generation in contractile cells. *J. Mech. Behav. Biomed. Mater.* **4**, 1683–1699. (doi:10.1016/j.jmbbm.2011.05.022)
26. Himpel G, Kuhl E, Menzel A, Steinmann P. 2005 Computational modelling of isotropic multiplicative growth. *Comput. Model. Eng. Sci.* **8**, 119–134. (doi:10.3970/cmes.2005.008.119)
27. Kuhl E. 2014 Growing matter: a review of growth in living systems. *J. Mech. Behav. Biomed. Mater.* **29**, 529–543. (doi:10.1016/j.jmbbm.2013.10.009)
28. Kuhl E. 2016 Biophysics: unfolding the brain. *Nat. Phys.* **12**, 533–534. (doi:10.1038/nphys3641)

29. Ben Amar M, Bordner A. 2017 Mimicking cortex convolutions through the wrinkling of growing soft bilayers. *J. Elast.* **19**, 213–238. (doi:10.1007/s10659-017-9622-9)
30. Menzel A, Kuhl E. 2012 Frontiers in growth and remodeling. *Mech. Res. Commun.* **42**, 1–14. (doi:10.1016/j.mechrescom.2012.02.007)
31. Ben Amar M, Jia F. 2013 Anisotropic growth shapes intestinal tissues during embryogenesis. *Proc. Natl Acad. Sci. USA* **110**, 10 525–10 530. (doi:10.1073/pnas.1217391110)
32. Ciarletta P, Balbi V, Kuhl E. 2014 Pattern selection in growing tubular tissues. *Phys. Rev. Lett.* **113**, 248101. (doi:10.1103/PhysRevLett.113.248101)
33. Moulton DE, Goriely A. 2011 Possible role of differential growth in airway wall remodeling in asthma. *J. Appl. Physiol.* **110**, 1003–1012. (doi:10.1152/japplphysiol.00991.2010)
34. Ciarletta P, Ben Amar M. 2012 Papillary networks in the dermal-epidermal junction of skin: a biomechanical model. *Mech. Res. Commun.* **42**, 68–76. (doi:10.1016/j.mechrescom.2011.12.001)
35. Zöllner AM, Buganza Tepole A, Kuhl E. 2012 On the biomechanics and mechanobiology of growing skin. *J. Theor. Biol.* **297**, 166–175. (doi:10.1016/j.jtbi.2011.12.022)
36. Göktepe S, Abilez OJ, Parker KK, Kuhl E. 2010 A multiscale model for eccentric and concentric cardiac growth through sarcomerogenesis. *J. Theor. Biol.* **265**, 433–442. (doi:10.1016/j.jtbi.2010.04.023)
37. Goriely A, BenAmar M. 2005 Differential growth and instability in elastic shells. *Phys. Rev. Lett.* **94**, 198103. (doi:10.1103/PhysRevLett.94.198103)
38. Garikipati K. 2009 The kinematics of biological growth. *Appl. Mech. Rev.* **62**, 030801. (doi:10.1115/1.3090829)
39. Chuong CJ, Fung YC. 1986 On residual stress in arteries. *J. Biomech. Eng.* **108**, 189–192. (doi:10.1115/1.3138600)
40. Budday S, Steinmann P, Goriely A, Kuhl E. 2015 Size and curvature regulate pattern selection in the mammalian brain. *Extreme Mech. Lett.* **4**, 193–198. (doi:10.1016/j.eml.2015.07.004)
41. Kröner E, Seeger A. 1959 Nicht-lineare Elastizitätstheorie der Versetzungen und Eigenspannungen. *Arch. Rat. Mech. Anal.* **3**, 97–119. (doi:10.1007/BF00284168)
42. Epstein M. 2015 Mathematical characterization and identification of remodeling, growth, aging and morphogenesis. *J. Mech. Phys. Solids* **84**, 72–84. (doi:10.1016/j.jmps.2015.07.009)
43. Ambrosi D, Guana F. 2007 Stress-modulated growth. *Math. Mech. Solids* **12**, 319–342. (doi:10.1177/1081286505059739)
44. Grillo A, Zingali G, Federico S, Herzog W, Giaquinta G. 2005 The role of material inhomogeneities in biological growth. *Theor. Appl. Mech* **32**, 21–38. (doi:10.2298/TAM0501021G)
45. Imatani S, Maugin GA. 2002 A constitutive model for material growth and its application to three-dimensional finite element analysis. *Mech. Res. Commun.* **29**, 477–483. (doi:10.1016/S0093-6413(02)00294-X)
46. Tiero A, Tomassetti G. 2014 On morphoelastic rods. *Math. Mech. Solids* **21**, 10. (doi:10.1177/1081286514546178)
47. Rice JR. 1971 Inelastic constitutive relations for solids: an internal-variable theory and its application to metal plasticity. *J. Mech. Phys. Solids* **19**, 433–455. (doi:10.1016/0022-5096(71)90010-X)
48. Goriely A. 2017 Five ways to model active processes in elastic solids: active forces, active stresses, active strains, active fibers, and active metrics. *Mech. Res. Commun.* **93**, 75–79. (doi:10.1016/j.mechrescom.2017.09.003)
49. Yavari A, Goriely A. 2012 Riemann–Cartan geometry of nonlinear dislocation mechanics. *Arch. Ration. Mech. Anal.* **205**, 59–118. (doi:10.1007/s00205-012-0500-0)
50. Yavari A, Goriely A. 2015 On the stress singularities generated by anisotropic eigenstrains and the hydrostatic stress due to annular inhomogeneities. *J. Mech. Phys. Solids* **76**, 325–337. (doi:10.1016/j.jmps.2014.12.005)
51. Yavari A, Goriely A. 2012 Weyl geometry and the nonlinear mechanics of distributed point defects. *Proc. R. Soc. A* **468**, 3902–3922. (doi:10.1098/rspa.2012.0342)
52. Yavari A, Goriely A. 2013 Riemann–Cartan geometry of nonlinear disclination mechanics. *Math. Mech. Solids* **18**, 91–102. (doi:10.1177/1081286511436137)
53. Angoshtari A, Yavari A. 2013 A geometric structure-preserving discretization scheme for incompressible linearized elasticity. *Comput. Methods Appl. Mech. Eng.* **259**, 130–153. (doi:10.1016/j.cma.2013.03.004)
54. Chow B, Lu P, Ni L. 2006 *Hamilton's Ricci flow*, vol. 77. Providence, RI: American Mathematical Society.
55. Skalak R, Farrow DA, Hoger A. 1997 Kinematics of surface growth. *J. Math. Biol.* **35**, 869–907. (doi:10.1007/s002850050081)
56. Chirat R, Moulton DE, Goriely A. 2013 Mechanical basis of morphogenesis and convergent evolution of spiny seashells. *Proc. Natl Acad. Sci. USA* **110**, 6015–6020. (doi:10.1073/pnas.1220443110)
57. Weickenmeier J, Fischer C, Carter D, Kuhl E, Goriely A. 2017 Dimensional, geometrical, and physical constraints in skull growth. *Phys. Rev. Lett.* **118**, 248101. (doi:10.1103/PhysRevLett.118.248101)
58. Ganghoffer J-F, Plotnikov PI, Sokołowski J. 2014 Mathematical modeling of volumetric material growth. *Arch. Appl. Mech.* **84**, 1357–1371. (doi:10.1007/s00419-014-0884-4)
59. Kafadar CB. 1972 On Ericksen's problem. *Arch. Ration. Mech. Anal* **47**, 15–27. (doi:10.1007/BF00252185)
60. Yavari A, Goriely A. 2016 The anelastic Ericksen problem: universal eigenstrains and deformations in compressible isotropic elastic solids. *Proc. R. Soc. A* **472**, 20160690. (doi:10.1098/rspa.2016.0690)
61. Tomasek JJ, Gabbiani G, Hinz B, Chaponnier C, Brown RA. 2002 Myofibroblasts and mechano-regulation of connective tissue remodelling. *Nat. Rev. Mol. Cell. Biol.* **3**, 349–363. (doi:10.1038/nrm809)
62. Baaijens F, Bouten C, Driessen N. 2010 Modeling collagen remodeling. *J. Biomech.* **43**, 166–175. (doi:10.1016/j.jbiomech.2009.09.022)
63. Barocas VH, Tranquillo RT. 1987 An anisotropic biphasic theory of tissue-equivalent mechanics: the interplay among cell traction, fibrillar network deformation, fibril alignment, and cell contract guidance. *J. Biomed. Eng.* **119**, 137–145. (doi:10.1115/1.2796072)
64. Driessen NJB, Peters GWM, Huyghe JM, Bouten DVD, Baaijens FPT. 2003 Remodeling of continuously distributed collagen fibres in soft connective tissues. *J. Biomech.* **36**, 1151–1158. (doi:10.1016/S0021-9290(03)00082-4)
65. Kuhl E, Holzapfel GA. 2007 A continuum model for remodeling in living structures. *J. Mater. Sci.* **42**, 8811–8823. (doi:10.1007/s10853-007-1917-y)
66. Baek S, Rajagopal KR, Humphrey JD. 2006 A theoretical model of enlarging intracranial fusiform aneurysms. *J. Biomech. Eng.* **128**, 142–149. (doi:10.1115/1.2132374)
67. Baek S, Valentin A, Humphrey JD. 2007 Biochemomechanics of cerebral vasospasm and its resolution. *Ann. Biomed. Eng.* **35**, 1498–1509. (doi:10.1007/s10439-007-9322-x)
68. Miller KS, Khosravi R, Breuer CK, Humphrey JD. 2015 A hypothesis-driven parametric study of effects of polymeric scaffold properties on tissue engineered neovessel formation. *Acta Biomater.* **11**, 283–294. (doi:10.1016/j.actbio.2014.09.046)
69. Gleason RL, Humphrey JD. 2004 A mixture model of arterial growth and remodeling in hypertension: altered muscle tone and tissue turnover. *J. Vasc. Res.* **41**, 352–363. (doi:10.1159/000080699)
70. Cheng JK, Stoilov I, Mecham RP, Wagenseil JE. 2013 A fiber-based constitutive model predicts changes in amount and organization of matrix proteins with development and disease in the mouse aorta. *Biomech. Model. Mechanobiol.* **12**, 497–510. (doi:10.1007/s10237-012-0420-9)
71. Cyron CJ, Aydin RC, Humphrey JD. 2016 A homogenized constrained mixture (and mechanical analog) model for growth and remodeling of soft tissue. *Biomech. Model. Mechanobiol.* **15**, 1389–1403. (doi:10.1007/s10237-016-0770-9)
72. Latorre M, Humphrey JD. 2018 A mechanobiologically equilibrated constrained mixture model for growth and remodeling of soft tissues. *ZAMM-J. Appl. Math. Mech.* **98**, 2048–2071. (doi:10.1002/zamm.v98.12)
73. Garikipati K, Arruda E, Grosh K, Narayanan H, Calve S. 2004 A continuum treatment of growth in biological tissue: the coupling of mass transport and mechanics. *J. Mech. Phys. Solids* **52**, 1595–1625. (doi:10.1016/j.jmps.2004.01.004)
74. Lemon G, King JR, Byrne HM, Jensen OE, Shakesheff KM. 2006 Mathematical modelling of engineered tissue growth using a multiphase porous flow mixture theory. *J. Math. Biol.* **52**, 571–594. (doi:10.1007/s00285-005-0363-1)

75. Ateshian GA, Ricken T. 2010 Multigenerational interstitial growth of biological tissues. *Biomech. Model. Mechanobiol.* **9**, 689–702. (doi:10.1007/s10237-010-0205-y)
76. Grillo A, Federico S, Wittum G. 2012 Growth, mass transfer, and remodeling in fiber-reinforced, multi-constituent materials. *Int. J. Non-Linear Mech.* **47**, 388–401. (doi:10.1016/j.ijnonlinmec.2011.09.026)
77. Rachev A, Gleason RL. 2011 Theoretical study on the effects of pressure-induced remodeling on geometry and mechanical non-homogeneity of conduit arteries. *Biomech. Model. Mechanobiol.* **10**, 79–93. (doi:10.1007/s10237-010-0219-5)
78. Wagenseil JE. 2011 A constrained mixture model for developing mouse aorta. *Biomech. Model. Mechanobiol.* **10**, 671–687. (doi:10.1007/s10237-010-0265-z)
79. Myers K, Ateshian GA. 2014 Interstitial growth and remodeling of biological tissues: tissue composition as state variables. *J. Mech. Behav. Biomed. Mater.* **29**, 544–556. (doi:10.1016/j.jmbbm.2013.03.003)
80. Wu J, Shadden SC. 2015 Coupled simulation of hemodynamics and vascular growth and remodeling in a subject-specific geometry. *Ann. Biomed. Eng.* **43**, 1543–1554. (doi:10.1007/s10439-015-1287-6)
81. Soares JS, Sacks MS. 2016 A triphasic constrained mixture model of engineered tissue formation under in vitro dynamic mechanical conditioning. *Biomech. Model. Mechanobiol.* **15**, 293–316. (doi:10.1007/s10237-015-0687-8)
82. Vernerey FJ. 2016 A mixture approach to investigate interstitial growth in engineering scaffolds. *Biomech. Model. Mechanobiol.* **15**, 259–278. (doi:10.1007/s10237-015-0684-y)
83. Braeu FA, Seitz A, Aydin RC, Cyron CJ. 2017 Homogenized constrained mixture models for anisotropic volumetric growth and remodeling. *Biomech. Model. Mechanobiol.* **16**, 889–906. (doi:10.1007/s10237-016-0859-1)
84. Hill M, Philp CJ, Billington CK, Tatler AL, Johnson SR, O'Dea RD, Brook BS. 2018 A theoretical model of inflammation- and mechanotransduction-driven asthmatic airway remodelling. *Biomech. Model. Mechanobiol.* **17**, 1451–1470. (doi:10.1007/s10237-018-1037-4)
85. Moulton DE, Goriely A. 2011 Circumferential buckling instability of a growing cylindrical tube. *J. Mech. Phys. Solids* **59**, 525–537. (doi:10.1016/j.jmps.2011.01.005)
86. Goriely A, Vandiver R, Destrade M. 2008 Nonlinear Euler buckling. *Proc. R. Soc. A* **464**, 3003–3019. (doi:10.1098/rspa.2008.0184)
87. Goriely A, Budday S, Kuhl E. 2015 Neuromechanics: from neurons to brain. *Adv. Appl. Mech.* **48**, 79–139. (doi:10.1016/bs.aams.2015.10.002)
88. Biot MA. 1963 Surface instability of rubber. *Appl. Sci. Res.* **12**, 168–182. (doi:10.1007/BF03184638)
89. Breid D, Crosby AJ. 2009 Surface wrinkling behavior of finite circular plates. *Soft Matter* **5**, 425–431. (doi:10.1039/B807820C)
90. Jia F, Ben Amar M. 2013 Theoretical analysis of growth or swelling wrinkles on constrained soft slabs. *Soft Matter* **34**, 8216–8226. (doi:10.1039/c3sm50640a)
91. Ben Amar M, Wu M, Trejo M, Atlan M. 2015 Morpho-elasticity of inflammatory fibrosis: the case of capsular contracture. *J. R. Soc. Interface* **12**, 20150343. (doi:10.1098/rsif.2015.0343)
92. Budday S *et al.* 2017 Mechanical characterization of human brain tissue. *Acta Biomater.* **48**, 319–34. (doi:10.1016/j.actbio.2016.10.036)
93. Landau LD, Lifshitz EM. 1970 *Statistical physics*. Oxford, UK: Pergamon Press.
94. Landau LD, Lifshitz EM. 1970 *Theory of elasticity*. Oxford, UK: Pergamon Press.
95. Destrade M, Saccomandi G, Vianello M. 2013 Proper formulation of viscous dissipation for nonlinear waves in solids. *J. Acoust. Soc. Am.* **133**, 1255–1259. (doi:10.1121/1.4776178)
96. Cyron CJ, Humphrey JD. 2014 Vascular homeostasis and the concept of mechanobiological stability. *Int. J. Eng. Sci.* **85**, 203–223. (doi:10.1016/j.ijengsci.2014.08.003)
97. Erlich A, Moulton DE, Goriely A. 2018 Are homeostatic states stable? Dynamical stability in morphoelasticity. *Bull. Math. Biol.* **81**, 3219–3244. (doi:10.1007/s11538-018-0502-7)
98. Latorre M, Humphrey JD. 2019 Mechanobiological stability of biological soft tissues. *J. Mech. Phys. Solids* **125**, 298–325. (doi:10.1016/j.jmps.2018.12.013)
99. Satha G, Lindström SB, Klarbring A. 2014 A goal function approach to remodeling of arteries uncovers mechanisms for growth instability. *Biomech. Model. Mechanobiol.* **13**, 1243–1259. (doi:10.1007/s10237-014-0569-5)
100. Wu J, Shadden SC. 2016 Stability analysis of a continuum-based constrained mixture model for vascular growth and remodeling. *Biomech. Model. Mechanobiol.* **15**, 1669–1684. (doi:10.1007/s10237-016-0790-5)
101. Schwartz MA, Vestweber D, Simons M. 2018 A unifying concept in vascular health and disease. *Science* **360**, 270–271. (doi:10.1126/science.aat3470)
102. BenAmar M, Goriely A. 2005 Growth and instability in elastic tissues. *J. Mech. Phys. Solids* **53**, 2284–2319. (doi:10.1016/j.jmps.2005.04.008)
103. Ambrosi D, Mollica F. 2002 On the mechanics of a growing tumor. *Int. J. Eng. Sci.* **40**, 1297–1316. (doi:10.1016/S0020-7225(02)00014-9)
104. Wisdom KM, Delp SL, Kuhl E. 2015 Use it or lose it: multiscale skeletal muscle adaptation to mechanical stimuli. *Biomech. Model. Mechanobiol.* **14**, 195–215. (doi:10.1007/s10237-014-0607-3)
105. Zöllner AM, Pok JM, McWalter EJ, Gold GE, Kuhl E. 2015 On high heels and short muscles: a multiscale model for sarcomere loss in the gastrocnemius muscle. *J. Theor. Biol.* **3065**, 301–310. (doi:10.1016/j.jtbi.2014.10.036)
106. Alarcon T, Byrne HM, Maini PK. 2003 A cellular automaton model for tumour growth in inhomogeneous environment. *J. Theor. Biol.* **225**, 257–274. (doi:10.1016/S0022-5193(03)00244-3)
107. Richardson WT, Holmes JW. 2016 Emergence of collagen orientation heterogeneity in healing infarcts and an agent-based model. *Biophys. J.* **110**, 2266–2277. (doi:10.1016/j.bpj.2016.04.014)
108. Checa S, Prendergast PJ. 2009 A mechanobiological model for tissue differentiation that includes angiogenesis: a lattice-based modeling approach. *Ann. Biomed. Eng.* **37**, 129–145. (doi:10.1007/s10439-008-9594-9)
109. Hywood JD, Hackett-Jones EJ, Landman KA. 2013 Modeling biological tissue growth: discrete to continuum representations. *Phys. Rev. E* **88**, 032704. (doi:10.1103/PhysRevE.88.032704)
110. Bear MF, Connors BW, Paradiso MA. 2007 *Neurosciences*. Philadelphia, PA: Lippincott Williams and Wilkins.
111. McMahon T. 1984 *Muscles, reflexes, and locomotion*. Princeton, NJ: Princeton University Press.
112. Keener J, Sneyd J. 2009 *Mathematical physiology*, 2nd edn. Berlin, Germany: Springer.
113. McNeil AR. 2003 *Principles of animal locomotion*. Princeton, NJ: Princeton University Press.
114. Vogel S. 1996 *Life in moving fluids: the physical biology of flow*, 2nd edn. Princeton, NJ: Princeton University Press.
115. Holmes P, Full RJ, Koditschek D, Guckhenheimer J. 2006 The dynamics of legged locomotion: models, analyses, and challenges. *SIAM Rev.* **48**, 207–304. (doi:10.1137/S0036144504445133)
116. Gray J, Lissmann HW. 1938 Studies in animal locomotion. *J. Exp. Biol.* **15**, 506–517.
117. Cicconofri G, DeSimone A. 2015 A study of snake-like locomotion through the analysis of a flexible robot model. *Proc. R. Soc. A* **471**, 20150054. (doi:10.1098/rspa.2015.0054)
118. DeSimone A, Tatone A. 2012 Crawling motility through the analysis of model locomotors: two case studies. *Eur. Phys. J. E* **35**, 85. (doi:10.1140/epje/i2012-12085-x)
119. Childress S. 1981 *Mechanics of swimming and flying*. Cambridge, UK: Cambridge University Press.
120. Arroyo M, Heltai L, Milan D, DeSimone A. 2012 Reverse engineering the euglenoid movement. *Proc. Natl Acad. Sci. USA* **109**, 17 874–17 879. (doi:10.1073/pnas.1213977109)
121. Rossi M, Cicconofri G, Beran A, Noselli G, DeSimone A. 2017 Kinematics of flagellar swimming in *Euglena gracilis*: helical trajectories and flagellar shapes. *Proc. Natl Acad. Sci. USA* **114**, 13 085–13 090. (doi:10.1073/pnas.1708064114)
122. Mogilner A, Oster G. 1996 Cell motility driven by actin polymerization. *Biophys. J.* **71**, 3030–3045. (doi:10.1016/S0006-3495(96)79496-1)
123. Cardamone L, Laio A, Torre V, Shahapure R, DeSimone A. 2011 Cytoskeletal actin networks in motile cells are critically self-organized systems synchronized by mechanical interactions. *Proc. Natl Acad. Sci. USA* **108**, 13 978–13 983. (doi:10.1073/pnas.1100549108)
124. Recho P, Truskinovsky L. 2016 Maximum velocity of self-propulsion for an active segment. *Math. Mech. Solids* **21**, 263–278. (doi:10.1177/1081286515588675)

125. Recho P, Jerusalem A, Goriely A. 2016 Growth, collapse, and stalling in a mechanical model for neurite motility. *Phys. Rev. E* **93**, 032410. (doi:10.1103/PhysRevE.93.032410)
126. Bergert M, Erzberger A, Desai RA, Aspalter IM, Oates AC, Charras G, Salbreux G, Paluch EK. 2015 Force transmission during adhesion-independent migration. *Nat. Cell Biol.* **17**, 524–529. (doi:10.1038/ncb3134)
127. Alberts B, Johnson A, Lewis J, Morgan D, Raff M, Roberts K, Walter P. 2014 *Molecular biology of the cell*, 6th edn. New York, NY: Garland Science.
128. Bearsted J. 1930 *The Edwin Smith surgical papyrus*, vol. 1. Chicago, IL: University of Chicago Press.
129. Xu G, Knutsen AK, Dikranian K, Kroenke CD, Bayly PV, Taber LA. 2010 Axons pull on the brain, but tension does not drive cortical folding. *J. Biomech. Eng.* **132**, 071013. (doi:10.1115/1.4001683)
130. Striedter GF, Srinivasan S, Monuki ES. 2015 Cortical folding: when, where, how, and why? *Annu. Rev. Neurosci.* **38**, 291–307. (doi:10.1146/annurev-neuro-071714-034128)
131. Ronan L *et al.* 2013 Differential tangential expansion as a mechanism for cortical gyrification. *Cereb. Cortex* **24**, 2219–2228. (doi:10.1093/cercor/bht082)
132. Garcia KE *et al.* 2018 Dynamic patterns of cortical expansion during folding of the preterm human brain. *Proc. Natl Acad. Sci. USA* **115**, 3156–3161. (doi:10.1073/pnas.1715451115)
133. Richman DP, Stewart RM, Hutchinson JW, Caviness VS. 1975 Mechanical model of brain convolutional development. *Science* **189**, 18–21. (doi:10.1126/science.1135626)
134. Bayly PV, Taber LA, Kroenke CD. 2014 Mechanical forces in cerebral cortical folding: a review of measurements and models. *J. Mech. Behav. Biomed. Mater.* **29**, 568–581. (doi:10.1016/j.jmbbm.2013.02.018)
135. Budday S, Steinmann P, Kuhl E. 2014 The role of mechanics during brain development. *J. Mech. Phys. Solids* **72**, 75–92. (doi:10.1016/j.jmps.2014.07.010)
136. Bayly P, Okamoto R, Xu G, Shi Y, Taber L. 2013 A cortical folding model incorporating stress-dependent growth explains gyral wavelengths and stress patterns in the developing brain. *Phys. Biol.* **10**, 016005. (doi:10.1088/1478-3975/10/1/016005)
137. Dervaux J, Ben Amar M. 2011 Buckling condensation in constrained growth. *J. Mech. Phys. Solids* **59**, 538–560. (doi:10.1016/j.jmps.2010.12.015)
138. Ciarletta P, Balbi V, Kuhl E. 2014 Pattern selection in growing tubular tissues. *Phys. Rev. Lett.* **113**, 248101. (doi:10.1103/PhysRevLett.113.248101)
139. Tallinen T, Chung JY, Rousseau F, Girard N, Lefèvre J, Mahadevan L. 2016 On the growth and form of cortical convolutions. *Nat. Phys.* **12**, 588–593. (doi:10.1038/nphys3632)
140. Budday S, Kuhl E, Hutchinson JW. 2015 Period-doubling and period-tripling in growing bilayered systems. *Philos. Mag.* **95**, 3208–3224. (doi:10.1080/14786435.2015.1014443)
141. Li B, Jia F, Cao Y, Feng X, Gao H. 2011 Surface wrinkling patterns on a core-shell soft sphere. *Phys. Rev. Lett.* **106**, 234301. (doi:10.1103/PhysRevLett.106.234301)
142. Jia F, Pearce SP, Goriely A. 2018 Curvature delays growth-induced wrinkling. *Phys. Rev. E* **98**, 033003. (doi:10.1103/PhysRevE.98.033003)
143. Chaudhury MK, Chakrabarti A, Ghatak A. 2015 Adhesion-induced instabilities and pattern formation in thin films of elastomers and gels. *Eur. Phys. J. A* **38**, 1–26. (doi:10.1140/epje/i2015-15082-7)
144. Vella D, Bico J, Boudaoud A, Roman B, Reis PM. 2009 The macroscopic delamination of thin films from elastic substrates. *Proc. Natl Acad. Sci. USA* **106**, 10 901–10 906. (doi:10.1073/pnas.0902160106)
145. Cao Y, Hutchinson JW. 2012 From wrinkles to creases in elastomers: the instability and imperfection-sensitivity of wrinkling. *Proc. R. Soc. A* **468**, 94–115. (doi:10.1098/rspa.2011.0384)
146. Holland MA, Miller KE, Kuhl E. 2015 Emerging brain morphologies from axonal elongation. *Ann. Biomed. Eng.* **43**, 1640–1653. (doi:10.1007/s10439-015-1312-9)
147. Stewart PS, Waters SL, El Sayed T, Vella D, Goriely A. 2016 Wrinkling, creasing, and folding in fiber-reinforced soft tissues. *Extreme Mech. Lett.* **8**, 22–29. (doi:10.1016/j.eml.2015.10.005)
148. Alawiye H, Goriely A, Kuhl E. 2019 Revisiting the wrinkling of elastic bilayers I: linear analysis. *Phil. Trans. R. Soc. A* **377**, 20180076. (doi:10.1098/rsta.2018.0076)
149. Hutchinson JW. 2013 The role of nonlinear substrate elasticity in the wrinkling of thin films. *Phil. Trans. R. Soc. A* **371**, 20120422. (doi:10.1098/rsta.2012.0422)
150. Filas BA, Xu G, Taber LA. 2013 Mechanisms of brain morphogenesis. In *Computer models in biomechanics* (eds GA Holzapfel, E Kuhl), pp. 337–349. Berlin, Germany: Springer.
151. Brau F, Vandeparre H, Sabbah A, Poulard C, Boudaoud A, Damman P. 2011 Multiple-length-scale elastic instability mimics parametric resonance of nonlinear oscillators. *Nat. Phys.* **7**, 56–60. (doi:10.1038/nphys1806)
152. Cao Y, Hutchinson JW. 2012 Wrinkling phenomena in neo-Hookean film/substrate bilayers. *J. Appl. Mech.* **79**, 031019. (doi:10.1115/1.4005960)
153. Fu YB, Cai ZX. 2015 An asymptotic analysis of the period-doubling secondary bifurcation in a film/substrate bilayer. *SIAM J. Appl. Math.* **75**, 2381–2395. (doi:10.1137/15M1027103)
154. Holland M, Budday S, Goriely A, Kuhl E. 2018 Symmetry breaking in wrinkling patterns: gyri are universally thicker than sulci. *Phys. Rev. Lett.* **121**, 228002. (doi:10.1103/PhysRevLett.121.228002)
155. Budday S, Steinmann P, Goriely A, Kuhl E. 2015 Size and curvature regulate pattern selection in the mammalian brain. *Extreme Mech. Lett.* **4**, 193–198. (doi:10.1016/j.eml.2015.07.004)
156. Verner S, Garikipati K. 2018 A computational study of the mechanisms of growth-driven folding patterns on shells, with application to the developing brain. *Extreme Mech. Lett.* **18**, 58–69. (doi:10.1016/j.eml.2017.11.003)
157. Genet M, Lee LC, Baillargeon B, Guccione JM, Kuhl E. 2016 Modeling pathologies of systolic and diastolic heart failure. *Ann. Biomed. Eng.* **44**, 112–127. (doi:10.1007/s10439-015-1351-2)
158. Sahli Costabal F, Choy JS, Sack KL, Guccione JM, Kassab GS, Kuhl E. 2019 Multiscale characterization of heart failure. *Acta Biomater.* **86**, 66–76. (doi:10.1016/j.actbio.2018.12.053)
159. Taber LA. 1995 Biomechanics of growth, remodeling, and morphogenesis. *Appl. Mech. Rev.* **48**, 487–545. (doi:10.1115/1.3005109)
160. Rachev A. 1997 Theoretical study of the effect of stress-dependent remodeling on arterial geometry under hypertensive conditions. *J. Biomech.* **30**, 819–827. (doi:10.1016/S0021-9290(97)00032-8)
161. Kuhl E, Maas R, Himpel G, Menzel A. 2007 Computational modeling of arterial wall growth. attempts towards patient-specific simulations based on computed tomography. *Biomech. Model. Mechanobiol.* **6**, 321–331. (doi:10.1007/s10237-006-0062-x)
162. Watton PN, Ventikos Y, Holzapfel GA. 2009 Modelling the growth and stabilization of cerebral aneurysms. *Math. Med. Biol.* **26**, 133–164. (doi:10.1093/imammb/dqp001)
163. Valentin A, Humphrey JD. 2009 Evaluation of fundamental hypotheses underlying constrained mixture models of arterial growth and remodeling. *Phil. Trans. R. Soc. A* **367**, 3585–3606. (doi:10.1098/rsta.2009.0113)
164. Latorre M, Humphrey JD. 2018 Modeling mechano-driven and immuno-mediated aortic maladaptation in hypertension. *Biomech. Model. Mechanobiol.* **17**, 1497–1511. (doi:10.1007/s10237-018-1041-8)
165. Buganza Tepole A, Gart M, Gosain AK, Kuhl E. 2014 Characterization of living skin using multi view stereo and isogeometric analysis. *Acta Biomater.* **10**, 4822–4831. (doi:10.1016/j.actbio.2014.06.037)
166. Rockey MD, Darwin BP, Hill JA. 2018 Fibrosis—a common pathway to organ injury and failure. *N. Engl. J. Med.* **372**, 1138–1149. (doi:10.1056/NEJMra1300575)
167. Ben Amar M, Wu M, Trejo M, Atlan M. 2015 Morpho-elasticity of inflammatory fibrosis: the case of capsular contracture. *J. R. Soc. Interface* **12**, 20150343. (doi:10.1098/rsif.2015.0343)
168. Bui JM, Perry T, Ren CD, Nofrey B, Teitelbaum S, Van Epps DE. 2015 Histological characterization of human breast implant capsules. *Aesthetic Plast. Surg.* **39**, 306–315. (doi:10.1007/s00266-014-0439-7)
169. Jiang Y, Li G-Y, Qian L-X, Hu X-D, Liu D, Liang S, Cao Y. 2015 Characterization of the nonlinear elastic properties of soft tissues using the supersonic shear imaging (SSI) technique: inverse method, ex vivo and in vivo experiments. *Med. Image Anal.* **20**, 97–111. (doi:10.1016/j.media.2014.10.010)
170. Folkman J, Hochberg M. 1973 Self-regulation of growth in three dimensions. *J. Exp. Med.* **138**, 745–753. (doi:10.1084/jem.138.4.745)
171. Greenspan H. 1972 Models for the growth of a solid tumor by diffusion. *Stud. Appl. Math.* **51**, 317–340. (doi:10.1002/sapm.v51.4)

172. Helmlinger G, Netti PA, Lichtenbeld HC, Melder RJ, Jain RK. 1997 Solid stress inhibits the growth of multicellular tumor spheroids. *Nat. Biotechnol.* **15**, 778–783. (doi:10.1038/nbt0897-778)
173. Netti PA, Berk DA, Swartz MA, Grodzinsky AJ, Jain RK. 2000 Role of extracellular matrix assembly in interstitial transport in solid tumors. *Cancer Res.* **60**, 2497–2503.
174. Cheng G, Tse J, Jain RK, Munn LL. 2009 Micro-environmental mechanical stress controls tumor spheroid size and morphology by suppressing proliferation and inducing apoptosis in cancer cells. *PLoS ONE* **4**, e4632. (doi:10.1371/journal.pone.0004632)
175. Stylianopoulos T. 2012 Causes, consequences, and remedies for growth-induced solid stress in murine and human tumors. *Proc. Natl Acad. Sci. USA* **109**, 101–115. (doi:10.1073/pnas.1213353109)
176. Montel F. 2011 Stress clamp experiments on multicellular tumor spheroids. *Phys. Rev. Lett.* **107**, 188102. (doi:10.1103/PhysRevLett.107.188102)
177. Monnier S, Delarue M, Brunel B, Dolega ME, Delon A, Cappello G. 2016 Effect of an osmotic stress on multicellular aggregates. *Methods* **94**, 114–119. (doi:10.1016/j.ymeth.2015.07.009)
178. Ambrosi D, Preziosi L. 2002 On the closure of mass balance models for tumor growth. *Math. Models Methods Appl. Sci.* **12**, 737–754. (doi:10.1142/S0218202502001878)
179. Roose T, Netti PA, Munn LL, Boucher Y, Jain RK. 2003 Solid stress generated by spheroid growth estimated using a linear poroelasticity model. *Microvasc. Res.* **66**, 204–212. (doi:10.1016/S0026-2862(03)00057-8)
180. Lanir Y. 1987 Biorheology and fluid flux in swelling tissues. I. Bicomponent theory for small deformations, including concentration effects. *Biorheology* **24**, 173–187. (doi:10.3233/BIR-1987-24210)
181. Ambrosi D, Pezzuto S, Riccobelli D, Stylianopoulos T, Ciarletta P. 2017 Solid tumors are poroelastic solids with a chemo-mechanical feedback on growth. *J. Elast.* **129**, 107–124. (doi:10.1007/s10659-016-9619-9)
182. McGrail DJ, McAndrews KM, Brandenburg CP, Ravikumar N, Kieu QMN, Dawson MR. 2015 Osmotic regulation is required for cancer cell survival under solid stress. *Biophys. J.* **109**, 1334–1337. (doi:10.1016/j.bpj.2015.07.046)
183. Simon DD, Humphrey JD. 2014 Learning from tissue equivalents: biomechanics and mechanobiology. In *Bio-inspired materials for biomedical engineering* (eds AB Brennan, CM Kirschner), pp. 281–308. New York, NY: John Wiley & Sons.
184. Bell E, Ivarsson B, Merrill C. 1979 Production of a tissue-like structure by contraction of collagen lattices by human fibroblasts of different proliferative potential in vitro. *Proc. Natl Acad. Sci. USA* **76**, 1274–1278. (doi:10.1073/pnas.76.3.1274)
185. Simon DD, Horgan CO, Humphrey JD. 2012 Mechanical restrictions on biological responses by adherent cells within collagen gels. *J. Mech. Behav. Biomed. Mater.* **14**, 216–226. (doi:10.1016/j.jmbbm.2012.05.009)
186. Ezra DG, Ellis JS, Beaconsfield M, Collin R, Bailly M. 2010 Changes in fibroblast mechanostat set point and mechanosensitivity: an adaptive response to mechanical stress in floppy eyelid syndrome. *Invest. Ophthalmol. Vis. Sci.* **51**, 3853–3863. (doi:10.1167/iovs.09-4724)
187. Hu JJ, Humphrey JD, Yeh AT. 2009 Characterization of engineered tissue development under biaxial stretch using nonlinear optical microscopy. *Tissue Eng. Part A* **15**, 1553–1564. (doi:10.1089/ten.tea.2008.0287)
188. Khosravi R, Miller KS, Best CA, Shih YC, Lee Y-U, Yi T, Shinoka T, Breuer CK, Humphrey JD. 2015 Biomechanical diversity despite mechanobiological stability in tissue engineered vascular grafts two years post-implantation. *Tissue Eng. Part A* **21**, 1529–1538. (doi:10.1089/ten.tea.2014.0524)
189. Loerakker S, Ristori T, Baaijens FP. 2015 A computational analysis of cell-mediated compaction and collagen remodeling in tissue-engineered heart valves. *J. Mech. Behav. Biomed. Mater.* **58**, 173–187. (doi:10.1016/j.jmbbm.2015.10.001)
190. Oomen PJA, Holland MA, Bouten CVB, Kuhl E, Loerakker S. 2018 Growth and remodeling play opposing roles during postnatal human heart valve development. *Sci. Rep.* **8**, 1235. (doi:10.1038/s41598-018-19777-1)
191. Oomen PJA *et al.* 2016 Age-dependent changes of stress and strain in the human heart valve and their relation with collagen remodeling. *Acta Biomater.* **29**, 161–169. (doi:10.1016/j.actbio.2015.10.044)
192. Mattheck C, Burkhardt S. 1990 A new method of structural shape optimization based on biological growth. *Int. J. Fatigue* **12**, 185–190. (doi:10.1016/0142-1123(90)90094-U)
193. Mattheck C. 1990 Design and growth rules for biological structures and their application to engineering. *Fract. Fatigue Eng. Mater. Struct.* **13**, 535–550. (doi:10.1111/ffe.1990.13.issue-5)